JOURNAL OF GEOPHYSICAL RESEARCH, VOL. 106, NO. E12, PAGES 33,333–33,349, DECEMBER 25, 2001

Structure, spectra, and mobility of low-pressure ices: Ice I, amorphous solid water, and clathrate hydrates at $T < 150$ K

J. Paul Devlin

Department of Chemistry, Oklahoma State University, Stillwater, Oklahoma

Abstract. Recent advances in the study of low-pressure water ices, including clathrate hydrates, are examined, highlighting aspects of modern science possibly related to the behavior of water ices in extraterrestrial environments. An effort has been made to identify properties of ice that are likely to be important in the conditions that exist in such environments and to review advances in understanding these properties. The basic science of crystalline ice I is relatively mature, but attention is given to concepts, such as point defects, which continue to evolve and which relate in an important manner to the low-temperature behavior of ice I as well as of amorphous ice and the clathrate hydrates. A concept of amorphous and microporous amorphous ice, developed in the early 1980s, is presented, but more recent characterizations are emphasized. Similarly, fundamental properties of clathrate hydrates are summarized and used in discussions of more recently appreciated characteristics that may be important in space science. Particular emphasis is placed on the formation, infrared spectroscopy, and behavior of clathrate hydrates in vacuo at temperatures below 150 K. The review closes with a section on the properties of ice nanoparticles, which have only recently emerged as a subject of molecular science. Modern experimental and theoretical studies of ice particles have focused on the infrared spectra and structure of the ice surface, and the interaction of the surface with molecular adsorbates. Since, with the exception of high-energy radiation, ice normally interacts with its environment through surface processes, such research may enlighten future studies.

1. Introduction

We begin by considering which fundamental properties of the low-pressure ices of water may aid in understanding extraterrestrial processes in which ice is a factor. Since highly varied conditions are known or can be imagined to exist, any restrictions are somewhat artificial. The conditions invoked here are low temperatures (10-150 K), very low to moderate pressures (0-1.0 bar) and the possible presence of other molecules. The forms of ice which will be discussed are suited to these conditions, namely, crystalline ice I, clathrate hydrates, and amorphous ice. Within these conditions the amorphous ice may be either compacted (amorphous solid water (ASW)) or microporous (porous amorphous solid water (PASW)), and the ice I may be either hexagonal or cubic. At a basic level, enumerated properties could include (1) the structure at the molecular level, including the local structure near a typical water molecule, the structure at the ice surface, and the structure at interfaces with adsorbates or other condensed substances, (2) the mobility of the water molecules of the ice at low temperatures, in particular the orientational mobility, (3) the stability or metastability of the ice phase, including certain relationships to molecular mobility, (4) the reactivity of ice toward other small molecules where reaction is identified with the making/breaking of strong hydrogen bonds, i.e., H bond chemistry, and (5) the mobility of other molecular species within the ice.

There are books and reviews that constitute an outstanding resource on the basic knowledge of icy substances [*Hobbs*, 1974; *Petrenko and Whitworth*, 1999; *Davidson*, 1972; *Davidson and Ripmeester*, 1984; *Devlin*, 1990]. Although most of that knowledge cannot be presented in this brief, broad-ranging review, these are the sources of many of the basic principles presented here. The intention is to first introduce basic concepts related to the properties listed above and then use those concepts in later discussions of the different ices. One immediate objective is to present terminology of bulk and surface structure, molecular level mobility, and spectra that allows us to describe these properties. Initially, images and the associated terminology will be presented in the context of crystalline ice I.

2. Language of the Properties of Ice I

Throughout, we will refer to ice I without distinguishing between ice Ic (cubic ice) and ice Ih (hexagonal ice), the two very similar crystalline forms of ice that occur at low pressures. Hexagonal ice is always the stable phase of water below 273 K, but cubic ice commonly forms and exists at temperatures below ~180 K or in a finely divided state over a greater temperature range [*Huang and Bartell*, 1995]. Apparently, cubic ice is metastable by < 50J/mol with respect to hexagonal ice [*Handa* et al., 1988]; and, except for very minor differences in the far-infrared region [*Bertie and Jacobs*, 1977], has an infrared spectrum indistinguishable from that of

Paper number 2000JE001301.
0148-0227/01/2000JE001301$09.00

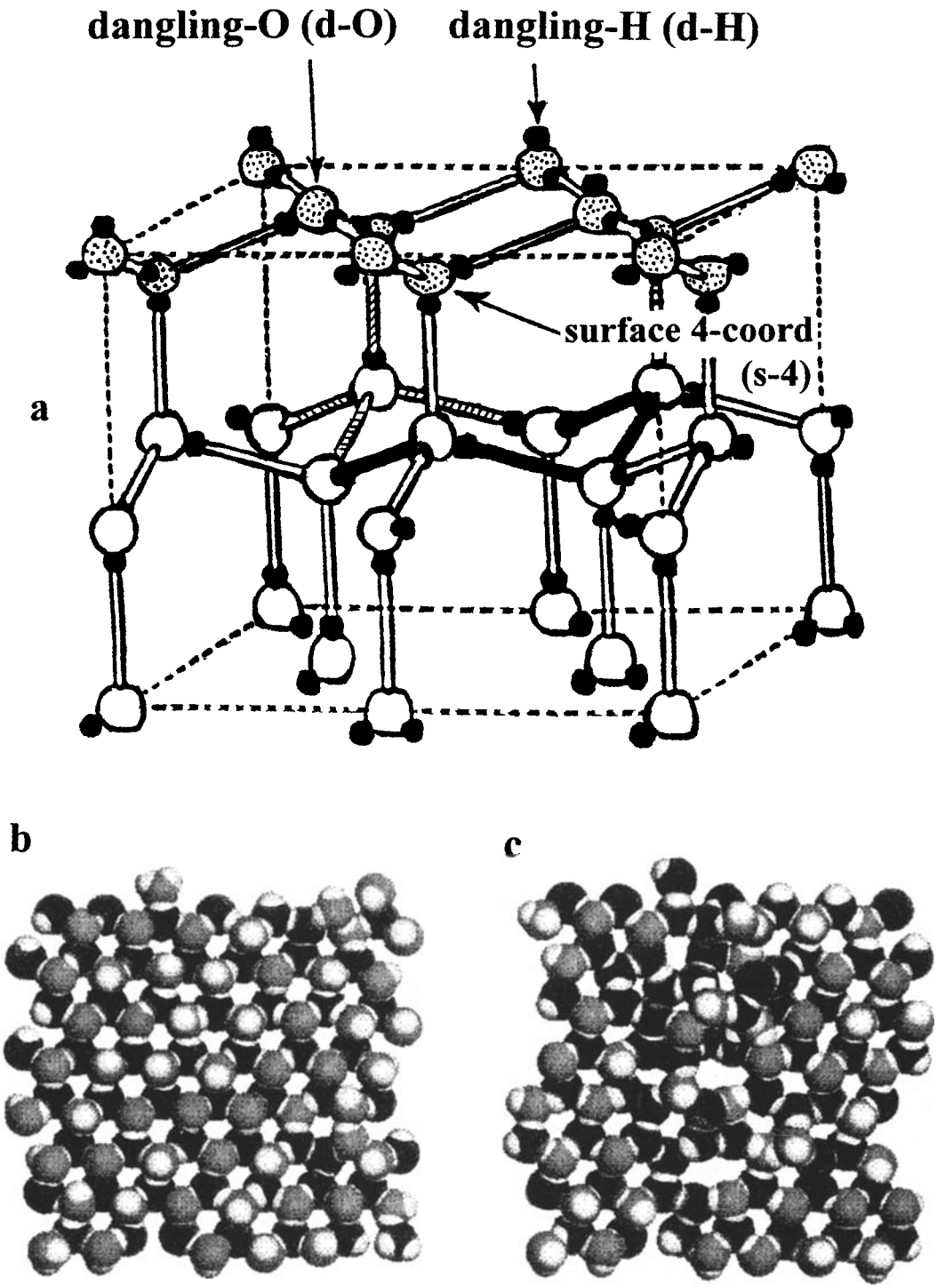

Figure 1. Figure 1a is a segment of the ice I structure with an interior bilayer (open circles for oxygen). A tetrahedral unit, emphasized by the crosshatched bonds, lies mainly in that bilayer. Two bonds of that unit are within a hexagonal ring that has thick solid lines representing the other four bonds. The large speckled circles represent oxygen of an oxygen-ordered, proton-disordered surface bilayer. Figure 1b is a view of the oxygen-ordered surface bilayer normal to the surface, with the light circles being the dangling hydrogen atoms and the shaded circles the dangling-oxygen. Figure 1c is the structure in figure 1b after relaxation by heating in a 103-ps trajectory followed by recooling to 46 K.

hexagonal ice. In the absence of diffraction data the phase of ice present is often uncertain.

2.1. Bulk Ice Structure

In a perfect cubic or hexagonal ice crystal the oxygen atoms form a periodic pattern which can be viewed as the result of stacking bilayers of water molecules, with each bilayer constructed from puckered hexagonal rings. Cubic ice differs from hexagonal ice only in the stacking sequence of the hexagonal bilayers. The structure, shown in Figure 1a, follows the ice rules (also called Bernal-Fowler rules), which means that each oxygen atom has four nearest-neighbor oxygen atoms arranged in a tetrahedral pattern, with a single H atom be-

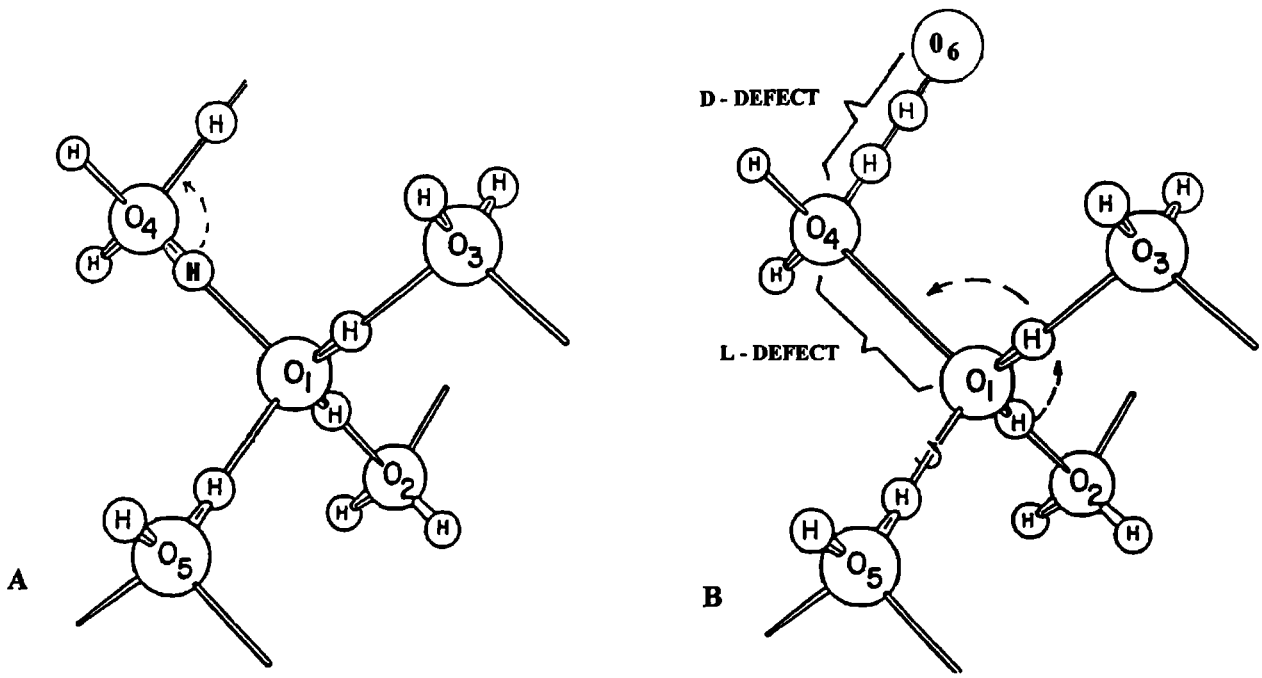

Figure 2. A representation of the formation and motion of the classic orientational point defects of ice I: (a) a random rotation of the O_4 water molecule generates L and D Bjerrum defects on neighbor hydrogen bonds, and (b), rotation about O_1 fills in the O_4 - - O_1 L defect and moves it to the O_1 - - O_2 position.

tween each near-neighbor oxygen pair. Each of these H atoms is chemically bonded to one oxygen and hydrogen bonded to another. Further, the water molecular unit is retained, as each oxygen is chemically bonded to two H atoms and hydrogen bonded to two others. Within a macroscopic piece of ice a great many arrangements of the hydrogen atoms, consistent with the ice rules, have essentially the same energy (i.e., near degenerate structures). One, the proton-ordered structure of ice XI, has the minimum energy [*Petrenko and Whitworth*, 1999, chap. 11]. Within most arrangements, there is no long-range correlation of the orientation of the water molecules, so the protons are disordered within structures that have a high degree of oxygen order.

2.2 Ice Mobility

Movement between nearly degenerate ice structures at low temperatures occurs through orientational mobility. A transition between structures could be imagined to require the making and breaking of several hydrogen bonds, which would require a high energy of activation. However, the activation energy is, in fact, quite low as determined from either dielectric relaxation or isotopic scrambling rates. The low activation energy (0.5-0.6 eV) can be understood in the context of orientational (Bjerrum) point defects. In pure crystalline ice the Bjerrum defects are formed in pairs with structures that can be imagined as either a missing hydrogen (L defect) or an extra hydrogen (D defect) along a near-neighbor oxygen-oxygen axis (Figure 2a). Either structure violates the ice rules near a particular lattice site, hence the term "point defect." An individual Bjerrum L defect, once formed as in Figure 2, may reorient many water molecules by moving from one oxygen-oxygen coordinate to another (Figure 2b) with a low energy of activation [*Kunst and Warman*, 1983]; that is, the L defect moves to position O_1- - O_2 by rotation of the O_1 molecule.

While the presence of a defect entity with a single extra or missing OH bond is likely to be correct, the Bjerrum model as shown in Figure 2 cannot be accurate beyond a cartoon level. There is considerable relaxation of the lattice structure in the vicinity of the defect. Recent computer simulations have given an updated molecular-level view of the structure and movement of these defects [*Podeszwa and Buch*, 1999]. Just as for the ionic point defects (H_3O^+ and OH^-), an equilibrium population of L and D defects reflects equal formation and recombination rates. Near the melting point the equilibrium population of point defects enables a high orientational mobility that allows rapid motion between structures and thus rapid dielectric relaxation or isotopic scrambling. However, the formation and mobilization energies of the Bjerrum defects are sufficiently high that both the number densities and mobility decrease rapidly with decreasing temperature. Consequently, orientational relaxation responses of ice I require of the order of an hour at 140 K [*Wooldridge and Devlin*, 1988]. As one consequence, the relaxation of pure ice to the stable form below 72 K, i.e., ordered ice XI, is not observed on a timescale of years.

2.3 Ice Surface Structure

Traditional discussions of crystalline ice have largely ignored the ice surface, with the exception of the question of the existence of a pseudoliquid layer at temperatures near the melting point [*Petrenko and Whitworth*, 1999, chap. 10]. However, low-temperature molecular-level studies of the ice surface have multiplied rapidly in the past decade. The ice of these recent investigations has been divided between thin crystalline films formed on metallic substrates [*Materer et al.*, 1995; *Su et al.*, 1998; *Braun et al.*, 1998; *Glebov et al.*, 1997] and nanocrystals having diameters in the range of 3 to ~100 nm [*Rowland et al.*, 1995; *Devlin and Buch*, 1995; *Buch et*

al., 1996; *Devlin and Buch*, 1997; *Hernandez et al.*, 1998; *Delzeit et al.* 1997a; *Devlin et al.*, 2000]. As one can imagine from the top surface layer of Figure 1a, termination of ice at a surface results in water molecules lacking the neighbors necessary for maintenance of the ice rules. Cleavage of ice parallel to the hexagonal bilayers, for example, will produce three subsets of surface-bilayer molecules: single-proton-donor water molecules with a dangling O-H (d-H molecules), double-donor molecules with a dangling lone pair of electrons (d-O molecules), and four-coordinated (saturated) molecules (s-4 molecules).

The d-H and d-O molecules, being three-coordinated, constitute the 50% of the surface sites at which the ice rules are violated (i.e., defects). These are the more reactive and more mobile sites of the surface and are of particular interest in studies of adsorbate ice interactions. Under careful low-T slow-deposition conditions a predominantly crystalline form of ice surface can apparently be obtained, as argued from helium diffraction measurements [*Glebov* et al., 1997, 2000]. However, computational studies [*Kroes*, 1992; *Devlin and Buch*, 1995] indicate that the oxygen-ordered surface (Figure 1b) of freestanding ice is nearly isoenergetic with an O-disordered structure characterized by a broad distribution of ring sizes (as opposed to hexagonal rings only) and a reduced population of three-coordinated molecules (see Figure 1c). The latter are replaced by four-coordinated molecules with a nearest-neighbor configuration strongly distorted from perfect tetrahedral symmetry. Any surface curvature is expected to further destabilize the crystalline surface. Our studies indicate that ice nanocrystal surfaces are O-disordered [*Buch et al.*, 1996; *Devlin et al.*, 2000]. This disordered form is likely to be characteristic of "generic" ice surfaces that are not prepared under special conditions favoring surface crystallinity.

2.4 Ice Spectra

The infrared spectra of water ices are often viewed as being made up of four different regions: the near-infrared region of overtone and combination bands; the 3-micron (3200 cm^{-1}) O-H stretch-mode region, the region, near 6.5 microns (1650 cm^{-1}), of the water-bending fundamental; and the lattice-mode region, extending through the far infrared but also including the lattice librational modes near 12 microns (800 cm^{-1}). Here we ignore the near-infrared spectra while focusing on the stretch and bend fundamentals along with the lattice modes.

Although the stretch modes of gas-phase water absorb quite weakly, the stretch modes of ice are characterized by a large infrared band intensity [*Bertie et al.*, 1989]. In addition to a downshift of frequency of 400-500 cm^{-1}, these modes experience a combined ~25-fold enhancement of the band intensity as a consequence of the formation of the strong hydrogen bonds of water ice. As is common for solid-state molecular systems, there is a resultant strong transition dipole-transition dipole intermolecular coupling of the stretch vibrations. This coupling determines the overall form of the observed infrared (and Raman) bands shown in the top spectrum of the inset of Figure 3. Because of this strong intermolecular coupling, subbands of the stretch modes range from below 3100 to near 3400 cm^{-1} (at 90 K) [*Whalley*, 1977; *Bergren and Rice*, 1982; *Wojcik* et al., 1993; *Buch and Devlin*, 1999]. Much of the breadth of the subbands originates from the proton-disordered nature of ice I, which breaks the crystal symmetry and activates vibrations for which the k vector (which measures the vibrational phase shift between neighboring molecules) is nonzero. There is also an exceptionally high sensitivity of the band positions to temperature, of the order of 0.2 $cm^{-1}K^{-1}$, which reflects the increasing strength of the H bonds with decreasing temperature [*Hagen et al.*, 1981; *Sivakumar et al.*, 1978]. Comparisons of spectra, such as in the inset of Figure 3, with interstellar ice spectra have often revealed a close analogy with the laboratory spectrum of PASW [*Hagen et al.*, 1981].

By contrast, pure ice I at low temperatures shows no infrared absorption that can be assigned to the molecular bending mode per se [*Bertie et al.*, 1969]. Rather, as is apparent in Figure 3a, a very broad weak band with a peak maximum near 1530 cm^{-1} is the only feature in the 6-micron range. This band is caused by excitation of states that are a thorough mix of the bending mode and the overtone of the librational mode. In essence, there is no bending-mode first excited state for ice I at low temperatures. This is less so for PASW, ASW, the ice surface, liquid water, or even H_2O molecules isolated intact in D_2O ice (J. P. Devlin and V. Buch, unpublished data, 2000). Rather, ice I at $T < 100$ K represents a unique limiting case of maximum overlap of the librational overtone with the bending mode. This results in the highly mixed excited states and a complete diffusion of the bending-mode band intensity.

In some respects the ice librational infrared band near 800 cm^{-1} resembles the stretch mode band. It is broad (~200 cm^{-1}) and reasonably intense; the two properties are interrelated, as the breadth reflects the intermolecular coupling of the librations of neighboring molecules, probably through a transition dipole mechanism. That intermolecular coupling is the cause of the band breadth is clear from the dramatic narrowing of the subbands of one isotopomer (HDO) isolated in the matrix of a second isotopomer (D_2O), as in Figure 3g. However, unlike the stretch modes, the frequency of the librational modes increases with increasing H bond strength, and there is a relative lack of structure of the infrared band (though the librational band of inelastic neutron scattering is highly structured [*Li*, 1996]).

3. Puzzles of the Vibrational Spectra of Ice I

The vibrational spectra of ice I have presented a number of puzzles, some of which have been resolved in recent years. These puzzles have included (1) the relative contribution of intermolecular and intramolecular coupling to the position of subbands in the stretch-mode infrared and Raman spectra; (2) the frequency of the water-molecule bending mode; (3) the origin of the dramatic difference between the bend-mode spectrum and that of liquid water; (4) the assignment of the weak, broad band near 4.5 microns (2250 cm^{-1}), (5) the origin of two well-spaced translational lattice bands in the neutron-scattering spectrum; and (6) the feasibility of observing point defects by spectroscopic methods.

The most successful approach to these puzzles has been through the use of isolated water molecule isotopomers within the ice of a second isotopomer. The approach gains much of its power from the mass difference inhibiting vibrational coupling of the dilute isotopomer with the neighbor molecules; so the spectra are simplified and any effect of decoupling is apparent. Since intramolecular and intermolecular coupling of the O-H (or O-D) oscillators are both eliminated for isolated HDO, the relative importance of the two types of coupling was not clear. This changed when it was discovered that crystal-

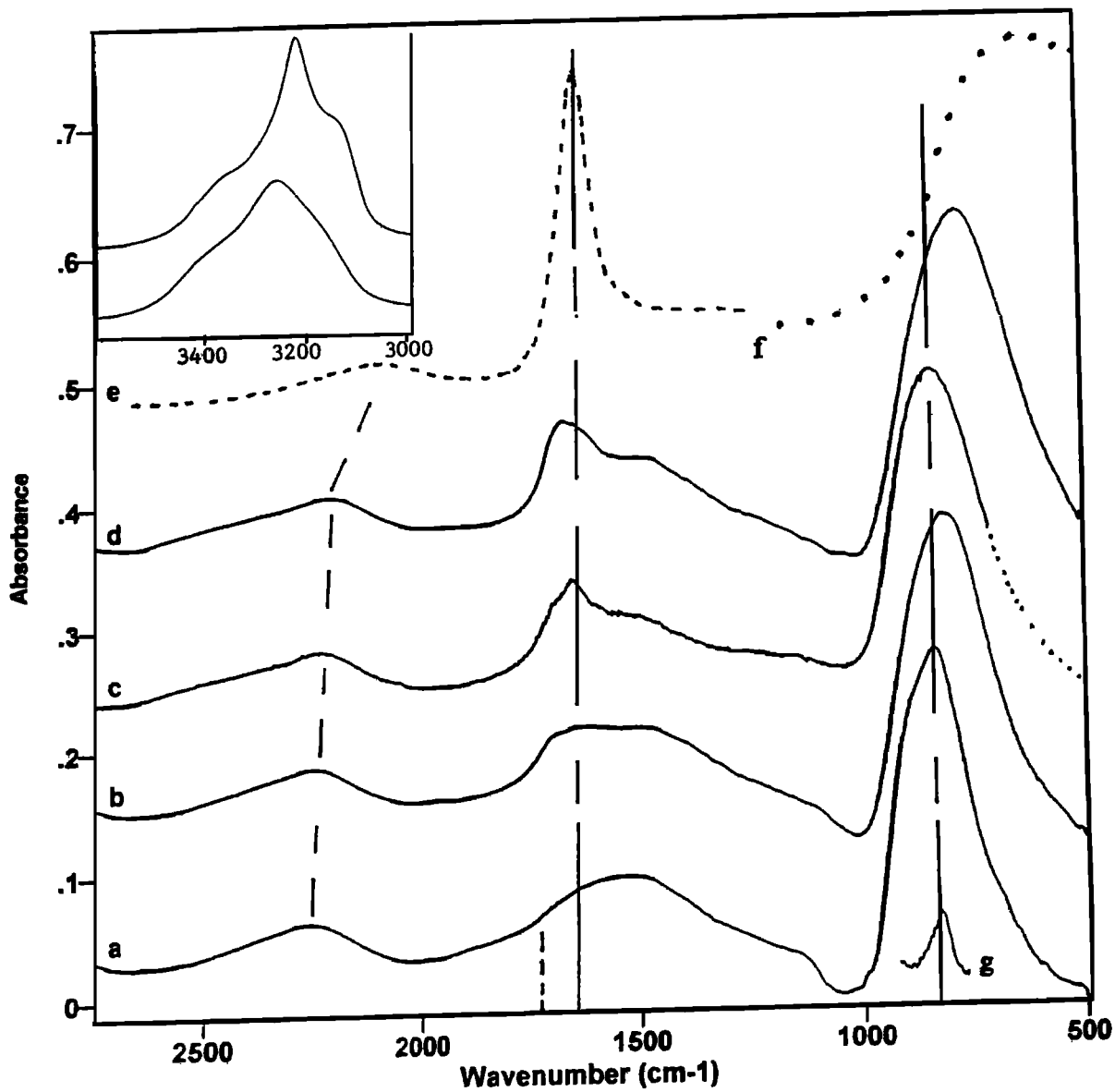

Figure 3. Infrared spectra for various phases of condensed H_2O: (a) crystalline ice at 12 K; (b) amorphous solid water (ASW) at 12 K after 12 K preparation and annealing at 130 K for 1 hour; (c) 100-K aerosol of 3-nm water clusters, (d) microporous ASW at 12 K after 12-K deposit; (e) H_2O(l) reproduced from *Bertie et al.* [1989]; and (f) H_2O (l; 274 K) plotted from *Pinckley et al.* [1977, Figure 4]. Curve g is for a few percent HDO in D_2O cubic ice. The absorbance scale applies only to a, b, and c. The dashed vertical line marks the position of the bend mode of H_2O isolated in D_2O cubic ice [*Ritzhaupt et al.*, 1980]. The inset shows the O-H stretch spectrum for (top) cubic ice and (bottom)ASW, both at 90 K.

line H_2O (D_2O) ice could be grown, with isolated intact D_2O (H_2O) molecules incorporated, by using "epitaxial" vapor deposition of a film at 120 K [*Ritzhaupt et al.*, 1978; *Ritzhaupt et al.*, 1980]. (It is argued in a recent report that the crystalline ice results not from epitaxial growth but from the crystalline sublayer serving as nucleation sites [*Dohnalek et al.*, 1999].) Pure ice produced at this low temperature contains no mobile ionic or orientational defects, so there is no mechanism for conversion of the D_2O to HDO (see section 3.6.).

3.1. Relative Intra and Intermolecular O-H Coupling Strengths

Comparison of the O-D stretch spectrum of isolated D_2O molecules with a spectrum of pure D_2O ice, as in Figure 4a, shows immediately the effect of the intermolecular coupling of the stretch modes in crystalline ice and also reveals the magnitude of the intramolecular coupling of D_2O in ice. The latter coupling gives a symmetric-asymmetric mode splitting of 52 cm^{-1} (after accounting for Fermi resonance with the overtone of the D_2O bend mode [*Sceats et al.*, 1979]). The variation of the intermolecular coupling effect, with the concentration of the two isotopomers, has also been displayed in Raman spectra over the full range of H_2O/D_2O percentages. These spectra have been shown to be compatible with computational results based on a dipole-dipole coupling model [*Wojcik et al.*, 1993]. These and related calculations have shown quite clearly that combination modes, often invoked in the past, make no serious contribution to the OH stretch-mode region.

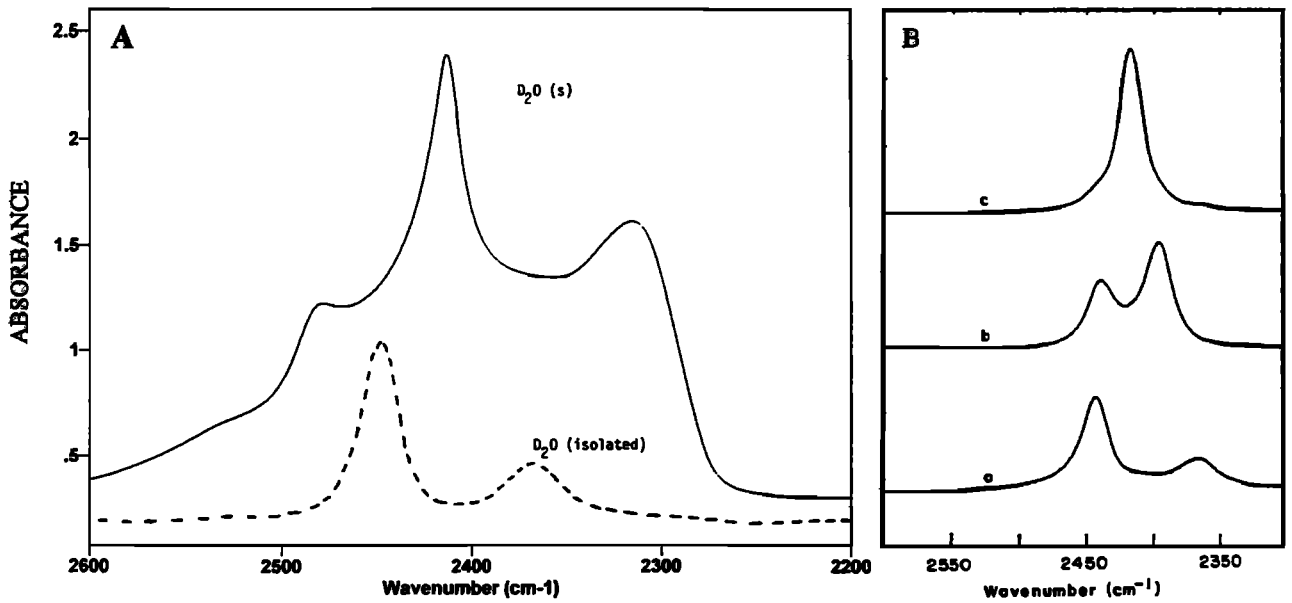

Figure 4. Figure 4a compares (top) the O-D stretch spectrum of pure D_2O ice I with (bottom) that of D_2O isolated in H_2O ice I, while Figure 4b includes (bottom) the latter spectrum with (top) that of isolated HDO and (middle) isolated neighbor-coupled $(HDO)_2$ units in H_2O ice.

3.2 Bend mode frequency of H_2O in ice I

The nature of the coupling of the bending mode with the overtone of the librational mode has not been investigated in any detail, but, again, the influence of the mixing of the states on the infrared spectrum is obvious from the spectrum of the H_2O isotopomer isolated in D_2O ice. As noted above, the bend band of pure H_2O ice I is not observable at low temperatures because of the mixing with the librational overtone. Because the librational fundamental band of the isolated H_2O is narrowed, the band of the overtone of the libration is narrowed dramatically. As a result, the "pure" bend-mode band of the isolated H_2O stands independently of the overtone band, appearing at 1740 cm^{-1} as a normal bend-mode absorption of ~50 cm^{-1} half width [*Ritzhaupt et al.*, 1980; *Devlin et al.*, 1986].

3.3. Ice I Bend Mode Versus that of H_2O(l)

The discussion of the last paragraph also extends to the mystery of the major difference between the bend-mode band of liquid water and that of crystalline ice. As shown in Figure 3e, a relatively narrow bend-mode band is prominent at 1645 cm^{-1} for liquid water. Why? This happens because no significant mixing with the overtone of the librational mode is expected (J. P. Devlin and V. Buch, unpublished data, 2000). Since the librational fundamental is at 570 cm^{-1} [*Pinkley et al*, 1977], the overtone is expected near 1100 cm^{-1}, far from the bending mode position. Though the second overtone of the libration may fall near the bend mode frequency, that overtone state would lack the proper symmetry to enable mixing with the first excited state of the bend mode. Consequently, the liquid-water bending band is not diffused from mixing with an overtone of the librational mode, a mixing that wipes out the bending band of ice I.

3.4 Assignment of the 4.5 Micron Ice I Band

The origin of the weak broad band of ice I near 2250 cm^{-1} has been controversial for some time [*Hagen et al.*, 1981]. It has variously been assigned as a combination of the bend-mode and librational-mode fundamentals [*Petrenko and Whitworth*, 1999, chap. 3] or as the second overtone of the librational mode. The former assignment was acceptable as long as the bend-mode fundamental frequency was unknown. However, with that frequency now available, from the dilute isotopomer band position, it is clear that the combination frequency with the libration (835 + 1735 = 2570 cm^{-1}) is much too high to produce the band at 2250 cm^{-1} The uncorrected frequency of the second overtone of the libration would also be too high, at 3 x 835 cm^{-1}. However, on the basis of the position of the first overtone near 1550 cm^{-1} (Figure 3a) the large anharmonicity of the librational mode is expected to place the second overtone near the band in question, so that is the favored assignment.

3.5 Origin of the Lattice Translational-Mode Doublet

The puzzle with respect to the translational lattice modes of ice I has a more recent origin. It has been known for some time that the Raman band near 230 cm^{-1} [*Scherer and Snyder*, 1977], and to a lesser extent the corresponding infrared band [*Bertie et al.*, 1969], has some structure on the high-frequency side that extends to near 310 cm^{-1}. This structure has been related to modes with longitudinal character [*Klug et al.*, 1991]. However, improved neutron-scattering spectra that show two very distinct bands, one at 28 meV (226 cm^{-1}) and a second at 38 meV (306 cm^{-1}), led to a proposal that the hydrogen bonds within ice are of two kinds, with the H bonds of the two sets differing in force constant by nearly a factor of 2 [*Li*, 1996]. However, the concept of such a large difference in

bond strength has not found acceptance, for reasons summarized by *Tse and Klug* [1995], and this particular puzzle may await a more definitive *resolution [Petrenko and Whitworth*, 1999, chap. 3] .

3.6 Point Defect Properties from Spectra

Because of very low populations, there have been no conclusive direct spectroscopic observations of either ionic or orientational point defects in crystalline ice. So observations of the existence/behavior of point defects have been indirect and largely macroscopic in nature, i.e., from dielectric and conductivity measurements. Though also indirect, a molecular-level probe of the effects of point-defect activity has been developed on the basis of isotopic exchange within ice samples having a nonequilibrium concentration of different isotopomers [*Collier et al.*, 1984; *Wooldridge and Devlin*, 1988].

Such samples, e. g., D_2O isolated in H_2O ice, contain an intrinsic spectroscopic probe of defect behavior. As shown in Figure 4b, not only do isolated D_2O and isolated HDO have characteristic spectra, but so does the HDO dimer (i.e., $(HDO)_2$) in which neighbor HDO share a D atom within a deuterium bond. If the classic view applies, ion defects move by proton hopping and the Bjerrum defects move by turning (Figure 2b)[*Petrenko and Whitworth*, 1999, chap. 6]; so passage of H_3O^+ can move a D atom from one end of an H bond to the other, while L defect motion can reorient water molecules that contain deuterium. Consequently, only the ion defect can convert isolated D_2O to $(HDO)_2$, which can subsequently be converted to isolated HDO only through the orientational motion of a Bjerrum defect. With each of the three deuterated species having a distinct infrared spectrum (Figure 4b), the effect of each type of defect can be observed independently.

The measurements of isotopic scrambling as a function of time and temperature have confirmed the view of ice point defects based on electrical measurements and embodied in the theories of Jaccard and Onsager [*Hobbs*, 1974]. The spectroscopic data have also shown that (1) H_3O^+ is immobilized in shallow traps at $T < 100$ K, which implies the existence of a trap-related activation energy for motion that onsets above 110 K [*Wooldridge and Devlin*, 1988], (2) orientational-defect activity within pure cubic ice is such that the average time between successive defect passages through a lattice site is about an hour at 140 K, and (3) the temperature dependence of the orientational motion is governed by an activation energy of 12.0 kcal $mole^{-1}$. The mobility of protons in ice below 190 K has recently been challenged [*Cowin et al.*, 1999], but proton hopping is the only feasible mechanism for the observed isotopic exchange, which onsets near 110 K for proton-enriched ice and near 135 K for pure ice. The insights to the orientational mobility of ice at cryogenic temperatures, as well as similar insights for ASW [*Fisher and Devlin*, 1995] and clathrate hydrates [*Richardson et. al.* 1985a], may aid in identification of processes and mechanisms that are feasible under extraterrestrial conditions (see section 8 on clathrate hydrate formation).

4. Advances in Understanding of Ice I

A large share of the recent advances in knowledge of the behavior of ice I at low temperatures has accompanied the numerous studies of (1) the nature of the ice surface and its interaction with adsorbates, (2) the nature of ultrathin films of crystalline ice on metal surfaces, and (3) the mechanism and extent of conversion of ice I to proton-ordered orthorhombic ferroelectric ice XI. We will focus on the ice surface and its interaction with adsorbates in section 10. Though of importance, both to basic science and the field of metal surface catalysis, the nature of thin ice films under the influence of a metal substrate is not directly relevant to most space science, it so will not be reviewed here. Similarly, though the temperature (<72 K) and pressure regime is appropriate, the topic of proton-ordered ice can be viewed as a secondary consideration of present-day space science (though the unusual defect activity of certain clathrate hydrates [*Suga et al.*, 1993] raises the possibility of proton ordering over extremely long periods at very low temperatures). Here a limited set of advances, with possible applicability to space science but not noted in the previous sections, is considered.

4.1 Infrared Optical Constants of Ice

There have been two quite recent investigations of the optical constants of crystalline ice I: one based on thin film Fourier transform infrared (FTIR) spectroscopic measurements [*Toon* et al.,1994] and the other on FTIR spectra of ice microcrystals in inert gas aerosols [*Clapp et al.*, 1995]. These studies have improved the available optical constant data of ice I in the infrared region, and the description of the aerosol results is particularly convincing. The latter results have also been used to emphasize the strong dependence of the optical constants on temperature. This dependence is not surprising, since the unusual magnitude of the temperature shifts of the stretch-mode (~0.2 cm^{-1} K^{-1}) and librational-mode bands of low pressure ices has been known for some time [*Sivakumar et al.*, 1978; *Hagen et al.*, 1981] and must be a consideration of careful studies of the ice spectra. For example, in observations based on difference spectra of ice, such as in the comparison of a bare ice spectrum with that of ice coated with an adsorbate, band shifts from temperature differentials greater than ~0.2 K will give rise to artifacts that dominate the spectra.

4.2 Modeling of the Ice Structure

The molecular-level modeling of liquid water has been a subject of intense study for some time. During the past several years the modeling of the structure and dynamics of ice has received increased attention with a particular interest in the surface region [*Kroes*, 1992; *Buch et al.*, 1996; *Devlin and Buch*, 1995; *Devlin et al.*, 2000]. Most of the activity has relied on the use of analytical pair-additive water potentials such as SPC, TIPS2, or TIP4P, as developed originally for liquid water. Recently, a polarizable potential was developed with the specific property that it reflects the lower energy of ordered ice XI [*Buch et al.*, 1998]; a property not found with the earlier analytical potentials. The analytical potentials permit detailed studies of large numbers of water molecules in proton-disordered ice configurations and have been applied to questions such as the existence of the liquid-like layer at the ice surface near the melting point, the structure of ultrathin films on metal surfaces [*Witek and Buch*, 1999] and large clusters at much lower temperatures, and the nature of the orientational defects in ice [*Podeszwa and Buch*, 1999].

Much attention was devoted to modeling of OH stretch spectra [*Wojcik et al.*, 1993; *Buch and Devlin*, 1999]. A unified model was developed for the interpretation of infrared and Raman spectra of H_2O and D_2O; the band shapes were shown to be determined by the interplay of the intermolecular (dipole-dipole) and intramolecular coupling between vibrations of bonds within the tetrahedral ice structure. The stretch mode excitations were shown to be delocalized over the entire system of oscillators for pure crystalline H_2O or D_2O ice but somewhat less so for amorphous ice.

Efforts have also been made to model ice structure and behavior within quantum mechanical frameworks [*Allouche*, 1999; *Bussolin et al.*, 1998]. Most such studies have used a limited segment of proton-ordered ice to address questions of behavior of adsorbates on the ice surface. However, an ab initio pseudopotential method has been used to generate the full vibrational density of states for proton-disordered ice I [*Morrison et al.*, 1997].

4.3 Water Molecule Diffusion in Ice I

The translational diffusion of water molecules in ice at temperatures <150 K has not been studied directly. However, elegant laser desorption methods, combined with nonequilibrium distributions of water isotopomers, have been used to gauge the self-diffusion of water molecules in ice thin films in the 153-170 K range [*Livingston et al.*, 1998]. These measurements showed a very rapid rise in mobility in this range corresponding to a high activation energy (17.0 kcal mol^{-1}). Because the observed diffusion was also much faster than expected from extrapolation of high-temperature bulk ice data, it was concluded that perturbations of the ice by the nearby metal substrate and vacuum interfaces create an excess of defects responsible for the high diffusivity. However, both the bulk and thin film results point to low self-diffusion rates below 150 K. This is consistent with the spectroscopic data for isotopic scrambling, which showed that scrambling rates for T < 150 K could be interpreted in terms of orientational and ionic point-defect mobility alone [*Wooldridge and Devlin*, 1988]. Extensive translational diffusion of water molecules would have seriously interfered with that analysis by joining orientational motion in eliminating neighbor HDO molecules (see above)

5. ASW and PASW Characteristics

There were a number of excellent spectroscopic [*Hagen et al.*, 1981, *Hagen and Tielens*, 1982; *Sivakumar et al.*, 1978] and theoretical studies [*Rice et al.*, 1983] of amorphous ice predating the mid-1980s that, together with the Brunauer, Emmett and Teller (BET) measurements of *Mayer and Pletzer* [1986], yielded a valid comprehensive image of bulk amorphous ice The surface area measurements first demonstrated a microporous nature with nanometer-sized pores that increase in number as the temperature of vapor deposition is reduced. For deposits prepared at 10 K, the infrared spectra revealed irreversible changes that occur during warming of the porous amorphous solid water (PASW), ultimately with formation of amorphous solid water (ASW) near 130 K. PASW was characterized as a high-energy structure with weaker H bonds, as evidenced by relatively high stretch-mode frequencies. Particularly in the bend-mode region, the spectra changed from water-like to ice-like during annealing (as in Figure 3). The annealing to ASW was considered to be complete at 130 K, and irreversible crystallization was apparent near 140 K. The vibrational spectra also showed an analogy between low-temperature ASW and warmer ice I, in terms of band positions, bandwidth, and response to changing temperatures.

The theoretical work identified ASW as a continuous random network of primarily four-coordinated water molecules [*Alben and Bouton*, 1975]. Theory also showed that intermolecular dynamical coupling, which dominates the vibrational spectra of ice I, remains a prime factor in the vibrational spectra of ASW (despite the loss of order in the positioning of the oxygen atoms). The effects on the O-D stretch spectrum of vibrational decoupling associated with isotopic dilution, for D_2O isolated in H_2O amorphous ice, confirmed the retention of strong intermolecular coupling within ASW and revealed the relative magnitude of the intermolecular and intramolecular coupling of the O-H oscillators [*Ritzhaupt and Devlin*, 1977; *Devlin*, 1990].

At the same time, there were uncertainties about some properties of ASW and PASW. No characteristics of the spectra had been directly tied to the microporosity of PASW, and there was no useful molecular-level model of PASW. The question of the existence of a glass transition of ASW near 130 K was highly controversial, and application of the concept of point defects to ASW, as in ice I and the clathrate hydrates, was unexplored. It was known that temperature and other conditions of deposition influenced the nature of the PASW that was deposited, but little was known about the specifics of the relation of deposition parameters to structure, porosity, or density.

6. Advances in Understanding of Amorphous Ice

6.1. ASW Glass Transition

That ASW, as well as the related substances hyperquenched glassy water and pressure-amorphized ice, undergoes a glass transition in the region of 135 K has been established through several calorimetric studies [*Hallbrucker et al.*, 1989]. There is less certainty about the fundamental nature of the reversible change that occurs upon warming through the transition temperature. The uncertainty resides in whether the transition is to a liquid form of water, with associated molecular translational mobility, or to ASW with orientational motion that connects numerous near-degenerate structures, as is thought to occur at the "glass transition" of ice I and the clathrate hydrates [Suga et al., 1993]. No molecular studies have documented translational diffusion of water in ASW near 135 K, though evidence of rapid diffusion near 155 K was found in isotopic scrambling as measured by mass spectrometric monitoring of desorbed water of ice ultrathin films [*Smith et al.*, 1997]. On the other hand, spectroscopic monitoring of isotopic scrambling revealed no evidence of translational diffusion below 125 K on a timescale of 10^5 seconds [*Fisher and Devlin*, 1995]. The results of the latter study did suggest that a useful analogy may be drawn between the functioning of defects in ASW and ice I. The study also confirmed [*Johari et al.*, 1991] that orientational diffusion of ASW at 115 K occurs at the same rate as for ice I at ~140 K. This increased orientational activity of ASW is consistent with its higher concentration of defects.

6.2. Spectroscopy and Modeling of PASW Pore Surfaces

Vibrational spectroscopic studies of the ice surface originated with the discovery that the water molecules at the surface of the nanopores of microporous amorphous ice produce infrared bands that are indicative of the nature of the surface sites [*Buch and Devlin*, 1991]. These data suggested that the microporosity of PASW could be monitored spectroscopically, a concept that has since been firmly established. Concurrently, simulations of the growth of large amorphous ice clusters gave initial molecular-level images of PASW that still apply [*Buch*, 1992]. The simulated clusters possessed highly convoluted surfaces with an incipient pore structure. The interior of the clusters was characterized by a range of water-ring sizes and coordination numbers, with bent H bonds and a high intrinsic density. An obvious connection between surface spectra and structure was found in the division of those molecules with dangling OH groups into subsets of two- and three-coordinated molecules.

Originally, the spectroscopic interest was centered on the behavior of the narrow high-frequency bands of the dangling OH bonds (or d-H sites) of surface water molecules. Subsequently, the response of the spectrum to adsorbates led to identification and use of an infrared band of 3-coordinated water with dangling electron lone pairs (or d-O sites: 3570 cm^{-1}) [Devlin and Buch, 1995]. In general, infrared spectroscopy and simulated structures/spectra of the **amorphous** ice surface have been informative of i) annealing effects on the ice (surface) structure, ii) the temperature range over which specific small molecules can diffuse through the ice, iii) the strength of interaction of adsorbates with the different surface sites, iv) the extent to which small molecules are trapped within the ice as the micropores collapse during annealing and v) the preference of HDO molecules, at the d-H sites, to form deuterium rather than hydrogen bonds.

PASW, when formed by deposition of pure water vapor at temperatures below ~30 K, was found to have an exceptionally large surface area characterized by the presence of both two- and three-coordinated d-H molecules as identified by the simulated structures and infrared spectra [*Rowland et al.*,1991; *Buch and Devlin*, 1991]. Titration of the surface sites, with small molecules such as N_2, indicated that more than 10% of the ice water molecules were at pore surfaces. Warming above 30 K caused rearrangement of the ice as evidenced by a gradual decrease in the population of two-coordinated sites (2748 cm^{-1}) over the range 30–60 K. Further warming, through the 60–120 K range, gradually eliminated the band of the three-coordinated d-H sites (2728 cm^{-1}) and signaled the collapse of the nanopores with the evolution of a continuous random network of four-coordinated molecules, i.e., ASW [*Devlin and Buch*, 1995; *Zondlo et al.*, 1997].

It is important to recognize that because of the pore structure, two different density concepts are applicable to PASW. There is the density exclusive of the pore volume, which here is referred to as intrinsic, and the overall, or global density, inclusive of the pore volume. Computer simulations confirmed the four-coordinated near-tetrahedral structure of ASW with a reduced intrinsic density and surface area compared to PASW [*Devlin and Buch*, 1995]. Electron diffraction data have similarly been interpreted in terms of a high intrinsic density for PASW that anneals to a more open ASW interior structure of lower intrinsic but greater global density [*Jenniskens and Blake*, 1994]. A general spectroscopic signal for conversion of D_2O PASW to ASW, during the warming from 12 to 120 K, is a transfer of considerable absorption intensity from above 2500 cm^{-1}, the surface-molecule mode region, to the region around 2400 cm^{-1} [*Devlin and Buch*, 1995]. More recent studies of the surface spectra of large water clusters indicate that most of this shift of infrared intensity results from the effective transfer of four-coordinated molecules from the surface to the interior of the ice as the pores collapse [*Devlin et al.*, 2000].

The ability of small molecules to diffuse into PASW was determined by coating the 12-K pure water deposits with a thin layer of the substance of interest. At 12 K, only H_2 and neon were observed to move into the ice pores. This was apparent from a slight shifting of the d-H bands as the adsorbates associated with the dangling groups. The presence of H_2 throughout the ice was also marked by the appearance of an infrared band of the ortho-H_2 stretch frequency [*Hixson et al.*, 1992] (from infrared activity induced by interaction with the ice surface). For other small molecules the system temperature was raised until a frequency shift of the d-H band, induced by association with the adsorbate molecules, was observed. In this manner, the temperatures at which N_2, O_2, CO, CH_4, and CF_4 access the entire pore surface of PASW, on a timescale of several minutes, were determined as 18, 22, 28, 34, and 54 K, respectively [*Rowland et al.*, 1991] (J. P. Devlin; unpublished data, 1998). In contrast, molecules such as acetylene, SO_2, HCN, and NH_3, do not readily access the pores at any temperature. At low temperatures, such substances lack a necessary mobility. At higher temperatures (i.e., above ~90 K), access is cut off by the partial collapse of the PASW pore structure.

These more strongly interacting adsorbate molecules, which cannot diffuse into the nanopores of PASW, are arguably of more interest than the small, weakly interacting molecules that readily coat the nanopore surfaces at low temperatures. To sidestep this limitation imposed by failure of adsorbates to diffuse into the pores, the PASW can be prepared with the potential adsorbate molecules premixed with the water vapor before deposition [*Sandford et al.*, 1988]. Tests with N_2, which can be adsorbed either by diffusion or by premixing in the water vapor, show that the results are the same provided the N_2 concentration is held below about ~10 mol %. Higher levels of N_2 cause a structural modification of the PASW, resulting in an increased surface area, as also happens with premixed argon [*Givan et al.*, 1996]. Clearly at some concentration of an additive and, in general, for strongly H-bonding substances, the PASW prepared from a premixed vapor will differ from normal PASW. Nevertheless, interesting and credible studies of unsaturated hydrocarbons [*Silva and Devlin*, 1994; *Allouche*, 1999] and halomethanes [*Holmes and Sodeau*, 1999] have been possible using that method. Similar spectroscopic results have been obtained for acetylene adsorbed directly on nanocrystals of ice as were determined for PASW by the use of a premixed vapor.

The simulated structures have revealed basically three types of sites on the nanopore surfaces of PASW similar to those shown for ice I in Figure 1: the d-H, d-O, and the s-4 (or surface four-coordinated) sites [*Buch*, 1992; *Hixson et al.*, 1992]. For ice nanocrystals the influence of adsorbate interaction with each type of site can be distinguished. However, the surface molecule bands for PASW are broader and less well de-

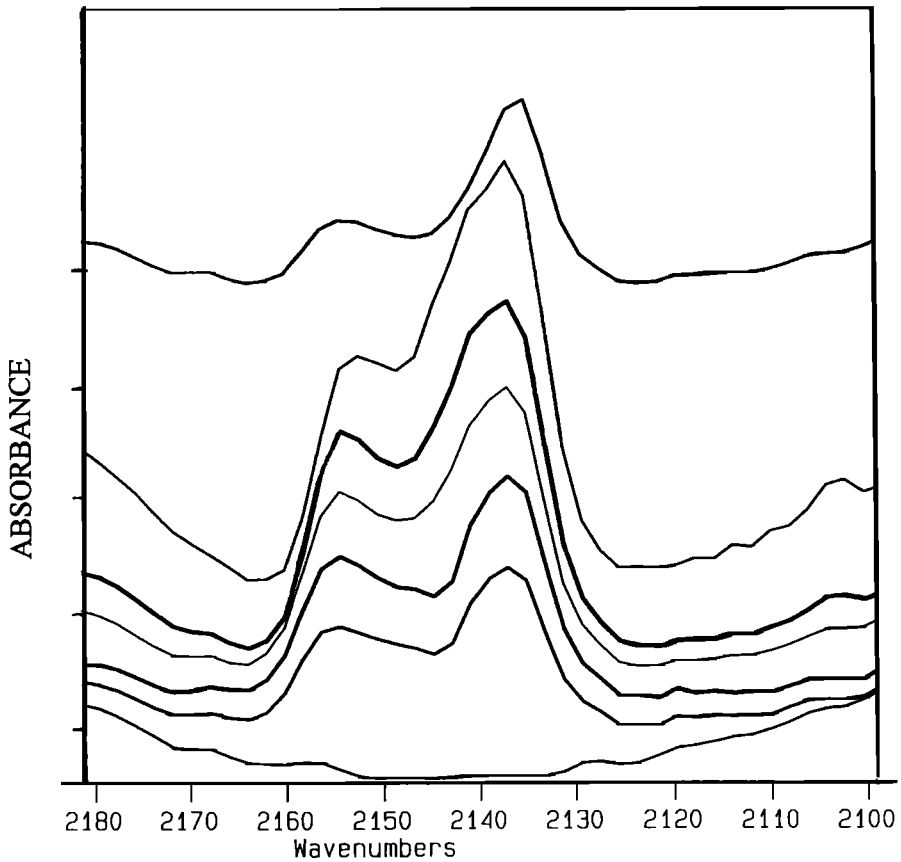

Figure 5. Spectra showing the two bands of CO [*Devlin*, 1992] adsorbed on the walls of PASW as a function of pressure, increasing from bottom to top: 0, 0.5, 1.0, 2.0, 8.0, and 16.0 torr at 85 K. The top spectrum is of the CO retained within the pores after exposure to a moderate vacuum for 3 hours.

fined, so only the shifting of the d-H band at 3697 cm^{-1} and the d-O band at 3570 cm^{-1} is apparent from the difference between spectra of the bare PASW and PASW coated with a weak adsorbate. The negative-going bands near 2700 and 2630 cm^{-1} in Figure 3b of *Rowland et al.* [1995] show the shifted band positions of the d-D and d-O molecules of D_2O PASW coated with weak adsorbates. The magnitude of the shift of a band can be viewed as a measure of the strength of the molecular interaction with the surface site. The largest reported shift is that induced by ammonia at the d-H sites (~650 cm^{-1}) of ice nanocrystals [*Delzeit et al.*, 1997b]. Numerous PASW shift values have been reported, and a table of values for 23 halomethanes exists [*Holmes and Sodeau*, 1999]. The analysis of the halomethane-induced d-H shifts, in terms of molecular ionization potentials and polarizabilities, identified the particular factors most responsible for the shifts.

The trapping of small molecules within the PASW nanopores presents complex questions [*Laufer et al.*, 1987]. If one starts by saturating the surface with a small molecular substance at low temperatures, warming will cause some of the adsorbate molecules to escape the ice as the pore structure collapses. Any molecules that remain after warming above ~90 K will be trapped within isolated nanopores as the ice is warmed toward the crystallization temperature. Some molecules become trapped even at 85 K as shown in Figure 5 for CO. Only upon crystallization will most of these molecules be rejected by the ice. However, it has been shown that if the population is kept artificially high by an overpressure imposed throughout the annealing range of the PASW, then, rather than crystallizing as ice I, a clathrate hydrate of the enclosed molecules is formed [*Consani and Pimentel*, 1987; *Mayer and Hallbrucker*, 1989].

It has been known for some time that if an HDO molecule has the choice of forming only one H bond as a donor molecule, the D donor rather than the H donor state is preferred because of zero-point vibrational energy differences. For example, HDO, with itself or with H_2O in an inert gas matrix at 10 K, forms almost exclusively the D-bonded dimer [*Engdahl and Nelander*, 1987]. For that reason, it is not surprising that the ice surface spectra indicate that an HDO molecule at a single-donor site on the ice surface (amorphous or crystalline) prefers the D-bonded orientation [*Rowland et al.*, 1991; *Devlin*, 2000]. Although the energy difference is minor (~0.6 kJ mol^{-1}), this preference is significant, with over two thirds of the surface molecules assuming that orientation at 120 K. Perhaps of more astrophysical interest is an insight gained from the relaxation of this orientational preference with temperature. No relaxation occurs for temperatures below 60 K, which identifies 60 K as the temperature of onset of rotational diffusion of surface water molecules on a timescale of 10^5 s.

6.3 Effect of Deposition Parameters on the Nature of Amorphous Ice

It has been recognized that differently structured amorphous ice deposits form under different conditions [*Mayer and Pletzer*, 1984] defined by substrate temperature, flow temperature, flow rate, flow source configuration, deposit thickness, sub-

strate character, and the presence or absence of a carrier gas or adsorbate vapor. Nevertheless, surprising differences have been noted in the nature of the amorphous ice formed with these parameters more or less standardized. This prompted a suggestion that the angle of impact of the molecules to the growing film at deposition might have a serious influence on the ice structure [*Westley et al.*, 1998]. A recent study of the effect of impact angle has confirmed that independent of temperature, the angle is a critical parameter in the determination of the porosity of the ice deposit [*Stevenson et al.*, 1999]. Large incidence angles give a high porosity, whereas no detectable porosity was noted for normal incidence sampling. Since the level of porosity affects the global density of the PASW, samples formed at normal incidence have a relatively high density. As noted [*Westley et al.*, 1998], this density may nevertheless be significantly less than the intrinsic density of highly porous ice produced, for example, by the random deposition angles of molecules of an ambient water vapor. It is the intrinsic density that is measured in electron diffraction experiments [*Jenniskens and Blake*, 1994]. The failure to note this critical difference between intrinsic and global density has been the source of some confusion.

Though the importance of deposition angle has been established, there appears to be a subtlety involved that is not resolved. The early spectroscopic studies of the surface of pure PASW used slow deposition from a single-nozzle source directed normal to a cooled plate held in a moderate vacuum [*Rowland et al.*, 1991]. Such conditions reproducibly generated PASW samples of high porosity, provided sample thickness was held under a micron. Thicker samples were known to detach from the substrate (often a salt window), at which time the ice, lacking thermal contact with the substrate, annealed and lost a high percentage of its porosity (B. Rowland and J. P. Devlin, unpublished data, 1991). The tendency to detach increases with a lowering of the deposition temperature and can be attributed to a high surface energy (instability) that increases with the porosity of the PASW. One can only conjecture why, in the absence of detachment, near-normal deposition under such conditions gives high porosity. It may be that after being adsorbed and released by warm surfaces within the cell, sufficient water molecules arrive at off-normal angles to give an effective off-normal impact angle.

7. Characteristics of Clathrate Hydrates

Clathrate hydrates (CHs) are solid solutions of guest molecules in an ice-like host lattice. There are two classic structural types, structure I and structure II, plus a more recently appreciated type, structure H. The structures are each characterized by the presence of relatively small molecules that stabilize the host structure while occupying well-defined cages. The emphasis here is on the structure I and II hydrates, as in the classic reviews by *Davidson* [1972] and *Davidson and Ripmeester* [1984]. The guest molecules of structure H are typically C4 hydrocarbons or larger, so that structural type is of particular importance in fuel science.

The great majority of CHs assume one of the two classic structures. Each structure has cages of two types, referred to as the large and small cages. The small cages of structures I and II are similar pentagonal dodecahedra suited to encage guests up to 0.50 nm in diameter, while the large cage of type I is a tetrakaidecahedron, with 12 pentagonal and two parallel hexagonal faces, receptive to molecules up to 0.55 nm in size. By comparison, the large type II cages, hexakaidecahedra with four hexagonal and 12 pentagonal faces, can accommodate guests with diameters < 0.66 nm. The ratio of the number of small to large cages is an important parameter. The type I structure has 46 water molecules per unit cell of the host lattice, which generate two small cages and six larger ones (1 to 3 ratio). By contrast, the type II structure has 136 water molecules per unit cell, which form 16 small cages and eight large ones (2 to 1 ratio). If the cages are fully occupied, the ratio of number of water molecules to guests is 5.75:1 for type I and 17:3 for type II hydrates. Generally, a guest molecule will prefer one cage size over the other, so the occupancy numbers in one cage may be much less than the maximum. For example, tetrahydrofuran forms a simple type II clathrate, but since the molecule is too large for the small cage, only the large cages are occupied. This results in a water:guest ratio of 17:1.

Generally, very small molecules prefer the type II structure because of the high small-to-large cage ratio; intermediately sized molecules, unable to occupy the small cages, prefer a type I structure; and larger molecules form type II structures, since they can fit only in the larger hexakaidecahedra. The ether four-membered-ring molecule trimethylene oxide, of intermediate diameter (0.55 nm), is an interesting guest, being capable of forming either the type I or II structures while occupying only the larger cages. Single guests form simple CHs. When a second guest is present, one guest may occupy exclusively the large and the other the small cages, forming what is called a double clathrate. If the two guests compete for cage occupancy, the result is a mixed clathrate. A single CH may include a number of different guests, a situation likely to arise in space environments.

Perhaps the most interesting CH parameter at low temperatures is the host-lattice orientational relaxation time that varies by orders of magnitude depending on the nature of the guest molecules [*Davidson and Ripmeester*, 1984]. Simple nonpolar molecules such as nitrogen, methane, and carbon dioxide form hydrates with long relaxation times, similar to that of pure ice I at the corresponding temperature. By contrast, proton-acceptor guests such as ethers, aldehydes, and ketones cause reductions in the relaxation times by factors as great as 10^4. Small populations of proton-acceptor guest molecules can dramatically increase the orientational mobility of a clathrate. Since orientational diffusion represents the primary mobility of pure icy substances below ~150 K, it is clear that tuning of the orientational relaxation rate by the guest molecule can have a dramatic influence on the hydrate behavior at cryogenic temperatures and thus on the behavior in space science. This concept underlies the discussion of the next section.

8. Formation of Clathrate Hydrates in vacuo at Cryogenic Temperatures

Historically, a large fraction of the molecular data for CHs has been derived from nuclear magnetic resonance measurements. This reflected the fact that the typical CH preparation, using high-pressure methodology at temperatures near the melting point of ice, produced the CHs in a bulk form not suited to optical spectroscopic measurements. A major change has occurred in the past two decades following the development of methods to prepare CHs in forms ideal for optical absorption experiments (along with an increasing awareness that Raman spectroscopic measurements are often feasible). The newer approaches, emphasized here, also yield CH forma-

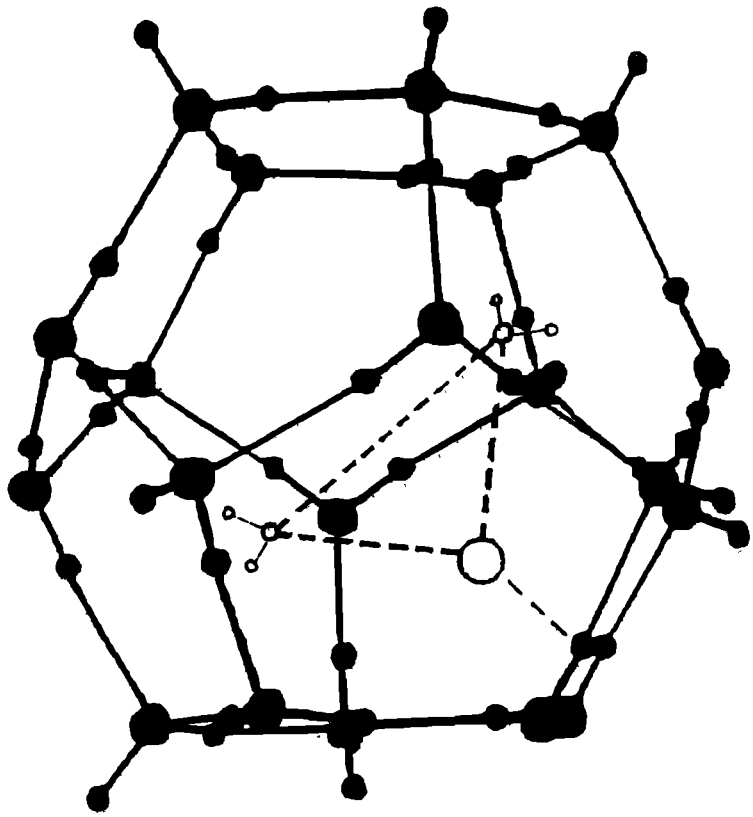

Figure 6. Representation, by a dashed line, of the interaction of the oxygen atom (open circle) of a proton-accepting molecule, ethylene oxide, with an OH group of the wall of a structure I clathrate hydrate small cage, with incipient defect formation. The thicker dashed lines indicate the ring of the small ether molecule.

tion/decomposition data over the temperature range of interest in space science.

The methods of preparation of crystalline CHs at T < 150 K in vacuo in a form ideal for FTIR measurements include the following:

1. An appropriate water:guest vapor mixture may be deposited as an amorphous thin film, followed by annealing in the 110-150 K range [*Bertie and Devlin*, 1983; *Blake et al.*, 1991; *Ripmeester et al.*, 1996]. The guest composition must normally include a proton-acceptor molecule such as a small ether, ketone or aldehyde; an exception being the simple type I CH of SO_2.

2. The crystalline CH may be vapor deposited directly from an appropriate water:guest vapor mixture at temperatures in the 100-150 K range. The guest composition must include a proton-acceptor molecule [*Richardson et al.*, 1985b].

3. Crystalline CHs of small "nonpolar" guests such as ethane, CO_2, cyclopropane, CH_3Cl, etc., may be vapor deposited but only with the help of a low percentage of guest molecules having proton-acceptor character [*Fleyfel and Devlin*, 1988].

4. CHs with nonpolar guest molecules may be grown epitaxially on CH films of proton-acceptor guests. Examples include CO_2 CHs of structure I and II [*Fleyfel and Devlin*, 1991].

5. Ice nanocrystal arrays may be converted to CH arrays using small proton-acceptor guest molecules with/without nonpolar guests [*Delzeit et al.*, 1997b; *Hernandez et al.*, 1998].

Because of the higher required temperatures, this list does not include methods of preparation of simple CHs of nonpolar molecules such as acetylene, N_2, and O_2 at temperatures near 180 K [*Consani and Pimental*, 1987; *Mayer and Hallbrucker*, 1989]. Also, the formation of CHs of nonpolar molecules at these or lower temperatures has been reported [*Thompson et al.*, 1987], but there has been no confirmatory molecular data; the hydrates, if present, are thought to have been limited to ultrathin surface films.

The point of greatest interest about the preparatory methods of the CHs at $T < 150$ K is the need for some presence of proton-acceptor guest molecules. Since, within an icy medium, such molecules are more tightly bound and less mobile than nonpolar molecules, their ability to induce the formation of CHs at these exceptionally low temperatures cannot be based on a greater translational mobility. The obvious difference between the properties of these and other guest molecules is the one mentioned earlier. Such proton-acceptor molecules convey orders-of-magnitude greater orientational mobility to the host-lattice system [*Davidson and Ripmeester*, 1984]. This added mobility has long been recognized and understood from a simple point-defect model. This model (Figure 6) presumes that a proton-donor guest molecule, on a highly transient basis, can hydrogen bond to an OH group of a water molecule of the wall of the clathrate cage [*Gough et al.*, 1968]. This disrupts the H bonding of the host system, creating an orientational defect resembling a Bjerrum L defect (Figure 2). On the basis of the relaxation rates, such action

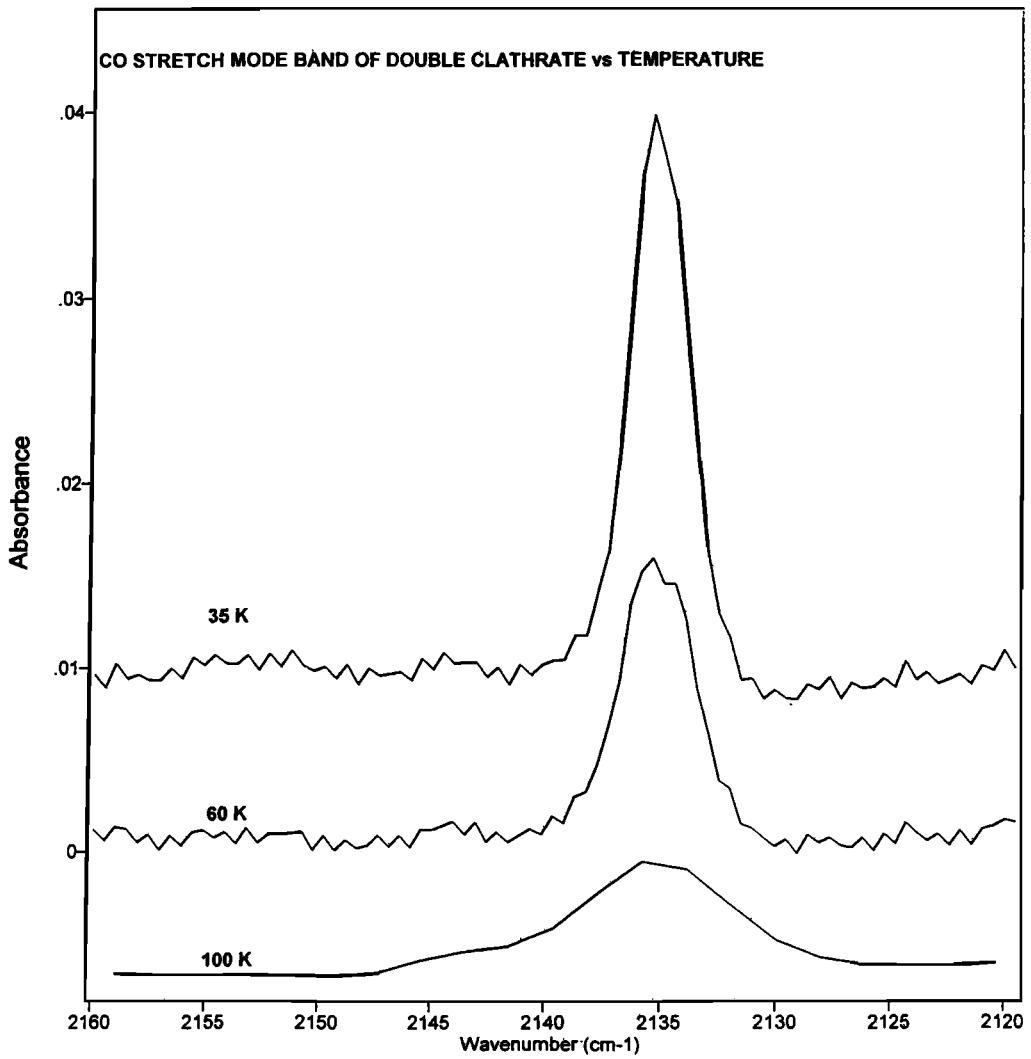

Figure 7. Infrared spectrum as a function of temperature of the stretch mode of CO in the small cages of a double CH with tetrahydrofuran. The absorbance scales of the spectra, measured at a resolution of 1 cm^{-1}, are the same. The sample was an array of CH nanocrystals formed by simultaneous uptake of CO and tetrahydrofuran by ice I nanocrystals at 120 K.

apparently increases the equilibrium concentration of (mobile) orientational defects within the host structure by orders of magnitude.

The action of the proton-acceptor guest is demonstrated in the complete conversion of ice nanocrystals to CHs containing large populations of nonpolar guest molecules. For example, although exposure of pure ice nanocrystals to CO_2 (g) for long periods at 120 K results in only adsorbed CO_2, this nonpolar guest rapidly fills the small cages of the tetrahydrofuran structure II CH at this temperature [*Hernandez et al.*, 1998]. Mobile defects, induced by the proton-acceptor guest, are imagined to loosen the CH structure, facilitating the diffusion of the CO_2, both into and away from the hydrate cages. A role of such defects in the rearrangement of CH structures has been shown theoretically [*Koga and Tanaka*, 1996]. The circumstantial evidence strongly suggests that it is this increased population of orientational defects that promotes the growth of CHs containing proton-acceptor guests at low temperatures. This provides a basis for regarding orientational-defect activity as a factor to be considered in low-temperature phase transitions of icy substances [*Wooldridge et al.*, 1987].

9. Spectroscopy of Clathrate Hydrates

The vibrational spectrum of a host lattice of a CH resembles that of ice I [*Bertie and Othen*, 1972]. However, the CHs have subsets of oxygen-oxygen near-neighbor distances of different lengths, ranging from about 2.74 to 2.82 angstroms [*Davidson*, 1972] with an average of ~2.79. The resulting range of water molecule environments is reflected in O-H stretch-mode bands of width intermediate to the bands of ice I and ASW, often shifted somewhat to higher frequencies versus ice I. The host bandwidths also reflect dynamical intermolecular coupling that is reduced by isotopic dilution [*Devlin*, 1990]. The spectra of guest molecules in CHs are generally distinctive but reflect only minor perturbations from the CH cage environments [*Bertie and Othen*, 1972]. However, at least two unique characteristics have been noted. The guest infrared bands tend to be broadened by large-amplitude rotational and translational motions, which are reduced by cooling. This can result in a dramatic increase in band peak heights as demonstrated in Figure 7 for CO in an array of nanocrystals of the double CH with tetrahydrofuran. A second

characteristic is higher stretch-mode frequencies for polyatomic guest molecules in the small cages versus the large cages [*Fleyfel and Devlin*, 1988].

Isotopic scrambling by active defects has been monitored spectroscopically following isolation of D_2O molecules in H_2O hydrates. The observed orientational-defect activity near 100 K for the CH of ethylene oxide was found to be comparable to that of ice I at 140 K [*Richardson et al.*, 1985a], which is consistent with the orders-of-magnitude more rapid relaxation rates of the CHs of proton acceptors as well as the glass transition temperatures noted by calorimetry [*Suga et al.*, 1993].

10. The Nature of Ice Nanoparticles

Laboratory spectroscopic study of ice nanoparticles represents a versatile approach to observation of ice behavior for a range of ice structures and environments. By working with particles in the 2-100 nm diameter range over temperatures ranging from 40 to 140 K, one can deliberately select particles with interior core structures that range from amorphous to crystalline and surface structures that vary from rough and energetic to smooth and relaxed [*Buch*, et. al., 1996]. However, the real advantage of nanoparticles in the laboratory resides in their high surface-to-volume ratio. This characteristic greatly facilitates the study of the spectra of the ice surface region [*Delzeit et al.*, 1997a; *Devlin and Buch*, 1995; *Devlin and Buch*, 1997], the surface interaction with a physical or chemical adsorbate [*Delzeit et al.*, 1997b; *Hernandez et al.*, 1998] and the conversion of ice to hydrates through H bond chemistry of the strongest adsorbates [*Devlin et al.*, 1999].

Observations and simulations of molecules on ice nanocrystal surfaces in the 40-140 K range have led to a categorization of a number of adsorbates and a clearer appreciation of the conditions required for the conversion of ice I to a new substance. Adsorbates have been categorized according to how they influence the three identifiable parts of an ice nanocrystal: the disordered surface, the strained subsurface, and the crystalline core. Weak adsorbates, such as H_2, N_2, CO, ethane, ethylene, argon, O_2, and CF_4, adapt themselves to the ice surface structure, sometimes engaging in weak specific interactions but commonly occupying sites at which multiple weak interactions dominate [*Hixson et al.*, 1992; *Buch and Devlin*, 1993], such as the centers of water rings [*Devlin and Buch*, 1995]. As in the case of PASW, such adsorbates cause minor shifts in the positions of the surface-water-molecule vibrational bands but have no significant impact on either the subsurface or core of ice nanocrystals. (Amorphous ice clusters, in the 1-nm range, are more pliable and may adjust their shape to best accommodate weak adsorbates (V. Buch, unpublished data, 2000).)

"Intermediate" adsorbates, such as SO_2, HCN, H_2S, and acetylene, for which the adsorbate-water bonding is comparable to the weakest surface H bonds between water molecules, cause large shifts of the infrared bands of the ice and are capable of breaking the weakest and most strained H bonds. (Many strained H bonds exist as a result of the surface reconstruction, which results in the surface disorder [*Buch et al.*, 1996].) With the strained H bonds replaced by bonds to the adsorbate, the surface reorders, causing much of the subsurface ice to relax to a form that appears spectroscopically as crystalline core ice. This adsorbate-induced relaxation, requiring a couple of hours at 125 K, allows recognition of the subsurface and its spectrum [*Delzeit et al.*, 1997a]. This relaxation, the simulated surface structures, and the comparison of experimental and simulated collective mode spectra for the adsorbate CF_4 [*Buch et al.*, 1996] all point to significant disorder in the top bilayer of ice nanocrystals.

At temperatures below 150 K the intermediate adsorbates cannot break the normal H bonds of ice, do not penetrate beyond the ice near-surface region, and do not nucleate a new solid phase. "Strong" adsorbates, such as NH_3, methanol, small ethers, and strong acids, for which the adsorbate-water bonding is comparable in strength to water-water bonding within ice, also reorder the ice surface and subsurface in the manner noted for intermediate adsorbates. However, strong adsorbates, at exposure levels beyond "surface saturation", are uniquely able to penetrate the ice and convert it to known hydrates [*Hernandez et al.*, 1998]. Since these processes involve the breaking and making of H bonds by molecular agents, each hydrate can be viewed as a product of "H bond chemistry." A strikingly broad range of solid forms can be obtained as a product of this chemistry, including ionic hydrates of acids, clathrate hydrates of ethers, and ammonia hydrates having molecular chain structures [*Delzeit et al.*, 1997b; *Uras and Devlin*, 2000].

Arrays of ice nanocrystals are particularly useful in the study of the conversion of ice to the amorphous or crystalline hydrates of the strong adsorbates. Because of the unusual surface-to-volume ratio of the particles, the timescale for a complete conversion is greatly compressed relative to that for bulk matter, or even thin films, which facilitates kinetic and mechanistic studies by FTIR spectroscopy, particularly at quite low temperatures. The several distinct stages of strong adsorbate interaction with ice, from initial uptake, through monolayer saturation, nucleation of the new phase, and, finally, complete conversion to a hydrate, are readily monitored at a single low temperature [*Uras and Devlin*, 2000]. This monitoring has made it particularly clear that before nucleation of a new hydrate phase can occur, the chemical activity of adsorbate molecules must surpass that of molecules tightly adsorbed in the first monolayer. This free-energy barrier for nucleation of a new phase may be a critical parameter of ice behavior in many environments.

It is interesting to compare the surface properties of ice nanocrystals to those of PASW, the other form of water ice with an inordinately large surface-to-volume ratio. Similarities and differences exist. Both have comparable amounts of the three types of surface sites we have labeled d-H, d-O, and s-4, but the position of the d-H and d-O bands are both ~5 cm^{-1} lower in frequency for the nanocrystals, and the shifts of band positions caused by adsorbate interactions are typically ~20% greater for PASW. H-bonding adsorbates do not diffuse to the pore surfaces of PASW, for reasons noted earlier, but readily coat the surfaces of nanocrystals in 3-D arrays. Weak adsorbates do not penetrate the nanocrystals, so, unlike for PASW, they are not occluded in the ice during subsequent annealing. Spectra showing the physical adsorption of H_2 at these different surfaces are presented in Figure 8, as one interesting example [*Hixson et al.*, 1992]. Again, similarities and differences are apparent. In both cases the H_2 molecule gains infrared activity, the ortho-H_2 adsorbs preferentially because of a stronger interaction with the surface [*Buch and Devlin*, 1993] and ortho to para conversion occurs over a matter of hours (perhaps from oxygen contamination). However, there are definite differences in H_2 bandwidths and positions.

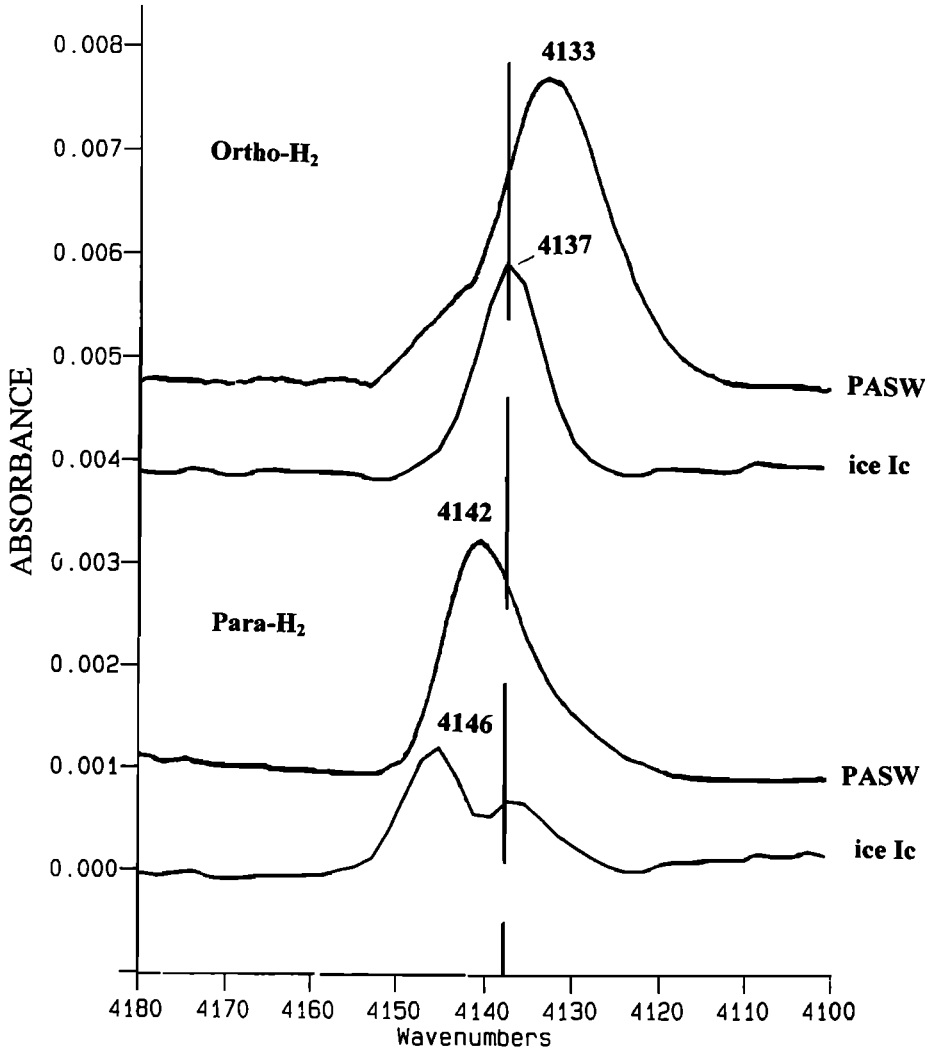

Figure 8. Infrared spectra of H_2 adsorbed on the ice surface at 20 K, as a function of time and the nature of the ice surface. The top two spectra were obtained immediately after exposure to the H_2 and show preferential adsorption of ortho-H_2 on PASW and cubic ice. In the bottom two spectra the bands of para-H_2, the stable form at low temperatures, are dominant.

11. Summary

Evidence is strong that water-rich solid matter is abundant throughout the universe. Reasonable conjecture of the properties of this matter can sometimes be derived from an understanding of simpler phases of solid water including ice I, ASW, amorphous solid solutions, and various crystalline clathrate hydrates, particularly from insights gained at the low temperatures and pressures that often characterize the extraterrestrial environments. Considerable progress in achieving this understanding has been made during the past several decades. The structural inclinations of solid water phases and the interaction of water with other molecules within condensed phases have been mapped to a considerable degree. These insights are useful for anticipation of levels of phase separation within icy solids in environments such as the cold interstellar molecular clouds. An important guiding principle is that the solubility of a second substance within ice I is meager unless the nucleation and growth of a hydrate phase, either crystalline or amorphous, occurs.

One area in which knowledge is particularly limited is the mobility of water and associated molecules within solid phases at low temperatures. It has been proposed here that below 150 K, molecular mobility is often dependent on orientational diffusion based on mobile orientational defects. This conjecture has a firm basis in data for the pure solid phases of water, including clathrate hydrates of proton-acceptor guests, but not for solid water solutions in general. Further, with one recent exception (*Uras and Devlin*, 2000), quantitative studies are largely lacking of the diffusivity of water or other molecules within low-temperature amorphous solid solutions. Fortunately, the increasing availability of reasonable global interaction potentials of water with other small molecules, combined with advances in simulation of molecular events, is beginning to yield insights that will, in time, apply to molecular diffusion in complex amorphous solutions.

Most of the knowledge of low-temperature icy water systems that is applicable to extraterrestrial science has been gained from bulk samples or relatively thick films. However, in real systems, ranging from Earth's stratosphere to the dark clouds of interstellar space, solid water often takes the form of nanoparticles or microparticles. Molecular processes within such systems tend to be dominated by events that occur within a few molecular layers of the particle surfaces. In part, this

reflects the containment of a considerable fraction of the substance within the surface and subsurface regions (e.g., half of the molecules in a 4-nm water particle are at the surface) and the arrival of new chemical agents at the surface. Equally important may be an exceptional molecular mobility associated with the surface region of particles. For example, for pure ice I the failure of the ice rules at the surface can be anticipated to enrich the subsurface region with (mobile) orientational defects. Thus the modeling of processes, using knowledge of bulk ice alone, presents a clear gamble. It is expected that data for water-rich molecular particles will be sought more aggressively in future laboratory and simulation studies.

Acknowledgment. Research support of the National Science Foundation under grant CHE-9983185 is gratefully acknowledged.

References

Alben, R., and P. Bouton, Continuous random network model for amorphous solid water, *Science, 187*, 430, 1975.

Allouche, A., Quantum studies of acetylene adsorption on ice surface, *J. Phys. Chem., 103*, 9150, 1999.

Bergren, M. S., and S. A. Rice, An improved analysis of the OH-stretching region of the vibrational spectrum of ice Ih, *J. Chem. Phys., 77*, 583, 1982.

Bertie, J. E., and J. P. Devlin, Infrared spectroscopic proof of the formation of the structure I hydrate of oxirane from annealed low-temperature condensate, *J. Chem. Phys., 78*, 6340, 1983. Bertie, J. E., and S. M. Jacobs, Far-infrared absorption by ices Ih and Ic at 4.3 K and the powder diffraction pattern of ice Ic, *J. Chem. Phys., 67*, 2445, 1977.

Bertie, J. E., and D. A. Othen, The infrared spectrum of ethylene oxide clathrate hydrate at 100 K between 4000 and 360 cm^{-1}, *Can. J. Chem., 51*, 1159, 1972.

Bertie, J. E., H. J. Labbe, and E. Whalley, Absortivity of Ice I in the Range 4000-30 cm^{-1}, *J. Chem. Phys., 50*, 4501, 1969.

Bertie, J. E., M. K. Ahmed, and H. H. Eysel, Infrared intensities of liquids. 5. Optical and dielectric constants, integrated intensities and dipole moment derivatives of H_2O and D_2O at 22 °C, *J. Phys. Chem. 93*, 2210, 1989.

Blake, D., L. Allamandola, S. Sanford, D. Hudgins, and F. Freund, Clathrate hydrate formation in amorphous cometary ice analogs in vacuo, *Science, 254*, 548, 1991.

Braun, J., A. Glebov, A. P. Graham, A. Menzel, and J. P. Toennies, Structure and phonons of the ice surface, *Phys. Rev. Lett., 80*, 2638, 1998.

Buch, V., Growth and structure of amorphous ice condensates: A computational study, II, *J. Chem. Phys., 96*, 3814, 1992.

Buch, V., and J. P. Devlin, Spectra of dangling OH bonds in amorphous ice: Assignment to 2- and 3-coordinated surface molecules, *J. Chem. Phys., 94*, 4091, 1991.

Buch, V., and J. P. Devlin, Preferential adsorption of ortho-H_2 with respect to para-H_2 on the amorphous ice surface, *J. Chem. Phys. 98*, 4195, 1993.

Buch, V., and J. P. Devlin, A new interpretation of the OH-stretch spectrum of ice, *J. Chem. Phys., 110*, 3437, 1999.

Buch, V., L. Delzeit, C. Blackledge. and J. P. Devlin, Structure of the ice nanocrystal surface from simulated versus experimental spectra of adsorbed CF_4, *J. Phys. Chem., 100*, 3732, 1996.

Buch, V., P. Sandler, and J. Sadlej, Simulations of H_2O solid, liquid and clusters, with an emphasis on ferroelectric ordering transition in hexagonal ice, *J. Phys. Chem. B, 102*, 8641, 1998.

Bussolin, G., S. Casassa, C. Pisani, and P. Ugliengo, *Ab initio* study of HCl and HF interaction with crystalline ice, I, Physical adsorption, *J. Chem. Phys, 108*, 9516, 1998.

Clapp, M. L., R. E. Miller, and D. R. Worsnop, Frequency-dependent optical constants of water ice obtained directly from aerosol extinction spectra, *J. Phys. Chem., 99*, 6326, 1995.

Collier, W. B., G. Ritzhaupt, and J. P. Devlin, Spectroscopically evaluated rates and energies for proton transfer and Bjerrum defect migration in cubic ice, *J. Phys. Chem., 88*, 363, 1984.

Consani, K., and G. C. Pimentel, Infrared spectra of the clathrate hydrates of acetylene and of acetylene/acetone, *J. Phys. Chem., 91*, 289, 1987.

Cowin, J. P., A. A. Tsekouras, M. J. Iedema, K. Wu, and G. B. Ellison, Immobility of protons in ice from 30 to 190 K, *Nature, 298*, 405, 1999.

Davidson, D. W., Clathrate Hydrates, in *Water, A Comprehensive Treatise.* vol. 2, edited by F. Franks, chap. 3, pp. 115-234, Plenum, New York, 1972.

Davidson, D. W., and J. A. Ripmeester, NMR, NQR and dielectric properties of clathrates, in *Inclusion Compounds,* vol. 3, edited by J. L. Atwood, J. E. D. Davies, and D. D. MacNicol, pp. 69-128, Academic, San Diego, Calif., 1984.

Delzeit, L., J. P. Devlin, and V. Buch, Structural relaxation rates near the ice surface: Basis for separation of the surface and subsurface spectra, *J. Chem. Phys., 107*, 3726, 1997a.

Delzeit, L., K. Powell, N. Uras and J. P. Devlin, Ice surface reactions with acids and bases, *J. Phys. Chem. B*, 101, 2327, 1997b.

Devlin, J. P., Vibrational spectra and point defect activities of icy solids and gas phase clusters, *Int. Rev. Phys. Chem., 9*, 29, 1990.

Devlin, J. P., Molecular interactions with icy surfaces: Infrared spectra of CO absorbed in microporous amorphous ice, *J. Phys. Chem., 96*, 6185, 1992.

Devlin, J. P., and V. Buch, Surface of ice as viewed from combined spectroscopic and computer modeling studies, *J. Phys. Chem., 99*, 16,534, 1995.

Devlin, J. P., and V. Buch, Vibrational spectroscopy and modeling of the surface and subsurface of ice and of ice-adsorbate interactions, *J. Phys. Chem., 101*, 6095, 1997.

Devlin, J. P., P. J. Wooldridge and G. Ritzhaupt, Decoupled isotopomer vibrational frequencies in cubic ice: A simple unified view of the Fermi diads of decoupled H_2O, HOD, and D_2O, J. Chem. Phys. 84, 6095, 1986.

Devlin, J. P., N. Uras, M. Rahman, and V. Buch, Covalent and ionic states of strong acids at the ice surface, *Isr. J. Chem., 39*, 261, 1999.

Devlin, J. P., C. Joyce, and V. Buch, Infrared spectra and structures of large water clusters, *J. Phys. Chem. A, 104*, 1974, 2000.

Devlin, J. P., Preferential deuterium bonding at the ice surface: A probe of surface water molecule mobility, *J. Chem. Phys., 112*, 5527, 2000.

Dohnalek, Z., R. L. Ciolli, G. A. Kimmel, K. P. Stevenson, R. S. Scott, and B. D. Kay, Substrate induced crystallization of amorphous solid water at low temperatures, *J. Chem. Phys., 110*, 5489, 1999.

Engdahl, A., and B. Nelander, On the relative stabilities of H- and D-bonded water dimers, *J. Chem. Phys., 86*, 1819, 1987.

Fisher, M., and J. P. Devlin, Defect activity in amorphous ice from isotopic exchange data: Insight into the glass transition, *J. Phys. Chem., 99*, 11,584, 1995.

Fleyfel, F., and J. P. Devlin, FT-IR spectra of 90 K films of simple, mixed, and double clathrate hydrates of trimethylene oxide, methyl chloride, carbon dioxide, tetrahydrofuran and ethylene oxide containing decoupled D_2O, *J. Phys. Chem., 92*, 631, 1988.

Fleyfel, F., and J. P. Devlin, Carbon dioxide clathrate hydrate epitaxial growth: Spectroscopic evidence for formation of the simple type-II CO_2 hydrate, *J. Phys. Chem., 95*, 3811, 1991.

Givan, A., A. Lowenschuss, and C. J. Nielsen, FTIR studies of CO-water complexes in argon matrices and in porous ice, *J. Chem. Soc. Faraday Trans., 92*, 4927, 1996.

Glebov, A., A. P. Graham, A. Menzel,and J. P. Toennies, Orientational ordering of two-dimensional ice on Pt(111), *J. Chem. Phys., 106*, 9382, 1997.

Glebov, A., A. P. Graham, A. Menzel, J. P. Toennies, and P. Senet, A helium atom scattering study of the structure and phonon dynamics of the ice surface, *J. Chem. Phys., 112*, 11,011, 2000.

Gough, S. R., E. Whalley, and D. W. Davidson, Dielectric properties of the hydrates of argon and nitrogen, *Can. J. Chem., 46*, 1673, 1968.

Hagen, W., and A. G. G. M. Tielens, The librational region in the spectrum of amorphous solid water and ice Ic between 10 and 140 K, *Spectrochim. Acta, Part A, 38*, 1089, 1982.

Hagen, W., A. G. G. M. Tielens, and J. M. Greenberg, The infrared spectra of amorphous solid water and ice Ic between 10 and 140 K, *Chem. Phys., 56*, 367, 1981.

Hallbrucker, A., E. Mayer, and G. P. Johari, Glass transition in pres-

sure-amorphized hexagonal ice: A comparison with amorphous forms made from the vapor and liquid, *J. Phys. Chem.*, *93*, 7751, 1989.

Handa, Y. P., D. D. Klug, and E. Whalley, Energies of the phases of ice at low temperature and pressure relative to ice Ih, *Can. J. Chem*, *66*, 919, 1988.

Hernandez, J., N. Uras, and J. P Devlin, Coated ice nanocrystals from water-adsorbate vapor mixtures: Formation of ether-CO_2 clathrate hydrate nanocrystals at 120 K, *J. Phys. Chem. B*, *102*, 4526, 1998.

Hixson, H. G., M. J. Wojcik, M. S. Devlin, J. P. Devlin, and V. Buch, Experimental and simulated vibrational spectra of H_2 absorbed in amorphous ice: Surface structures, energetics and relaxations, *J. Chem. Phys*, *97*, 753, 1992.

Hobbs, P. V., *Ice Physics*, Clarendon, Oxford, England, 1974.

Holmes, N. S., and J. R. Sodeau, A study of the interaction between halomethanes and water-ice, *J. Phys. Chem. A*, *103*, 4673, 1999.

Huang, J., and L. S. Bartell, Kinetics of homogeneous nucleation in the freezing of large water clusters, *J. Chem. Phys.*, *99*, 3924, 1995.

Jenniskens, P., and D. F. Blake, Structural transitions in amorphous water ice and astrophysical implications, *Science*, *265*, 753, 1994.

Johari, G. P., A. Hallbrucker, and E. Mayer, The dielectric behavior of vapor-deposited amorphous solid water and of its crystalline forms, *J. Chem. Phys.*, *95*, 2955, 1991.

Klug, D. D., J. S. Tse, and E. Whalley, The longitudinal-optic-transverse-optic mode splitting in ice Ih, *J. Chem. Phys.*, *95*, 7011, 1991.

Koga, K., and H. Tanaka, Rearrangement dynamics of the hydrogen-bonded network of clathrate hydrates encaging polar guest, *J. Chem. Phys.*, *104*, 263, 1996.

Kroes, G.-J., Surface melting of the (0001) face of TIP4P ice, *Surf. Sci.*, *275*, 365, 1992.

Kunst, M., and J. M. Warman, Nanosecond time-resolved conductivity studies of pulse-ionized ice, 2, The mobility and trapping of protons, *J. Phys. Chem.*, *87*, 4093, 1983.

Laufer, D, E. Kochavi, and A. Bar-Nun, Structure and dynamics of amorphous water ice, *Phys. Rev. B Condens Matter*, *36*, 9219, 1987.

Li, J., Inelastic neutron scattering studies of hydrogen bonding in ices, *J. Chem. Phys.*, *105*, 6733, 1996.

Livingston, F. E., G. C. Whipple, and S. M. George, Surface and bulk diffusion of HDO on ultrathin single-crystal ice multilayers on Ru(001), *J. Chem. Phys.*, *108*, 2197, 1998.

Materer, N., U. Starke, A. Barbieri, M. A. Van Hove, G. A. Somorjai, G. J. Kroes, and C. Minot, Molecular surface structure of a low-temperature ice Ih (0001) crystal, *J. Phys. Chem.*, *99*, 6267, 1995.

Mayer, E., and A. Hallbrucker, Unexpectedly stable nitrogen and oxygen clathrate hydrates from vapor deposited amorphous solid water, *J. Chem. Soc. Chem. Comm.*, *12*, 749, 1989.

Mayer, E., and R. Pletzer, Polymorphism in vapor deposited amorphous solid water, *J. Chem. Phys. 80*, 2939, 1984.

Mayer, E., and R. Pletzer, Astrophysical implications of amorphous ice-A microporous solid, *Nature*, *319*, 298, 1986.

Morrison, I., J.-C. Li, S. Jenkins, S. S. Xantheas, and M. C. Payne, Ab-initio total energy studies of the static and dynamical properties of ice Ih, *J. Phys. Chem. B*, *101*, 6146, 1997.

Petrenko, V. F., and R. W. Whitworth (Eds.), *Physics of Ice*, Oxford Univ. Press, New York, 1999.

Pinkley, L. W., P. P. Sethna, and D. Williams, Optical constants of water in the infrared: Influence of temperature, *J. Opt. Soc. Am.*, *67*, 494, 1977.

Podeszwa, R., and V. Buch, Structure and dynamics of orientational defects in ice, *Phys. Rev Lett.*, *83*, 4570, 1999.

Rice, S. A., M. S Bergren, A. C. Belch, and G. Nielson, A theoretical analysis of the OH stretching spectra of Ice Ih, liquid water and amorphous solid water, *J. Phys. Chem.*, *87*, 4295, 1983.

Richardson, H. H., P. J. Wooldridge, and J. P. Devlin, Determination of proton-transfer rates and energetics for the clathrate hydrate of oxirane by FT-IR spectroscopy, *J. Phys. Chem.*, *89*, 3552, 1985a.

Richardson, H. H., P. J. Wooldridge, and J. P. Devlin, FT-IR spectra of vacuum deposited clathrate hydrates of oxirane, H_2S, THF and ethane, *J Chem. Phys, 83*, 4387, 1985b.

Ripmeester, J A, L. Ding, and D. D. Klug, A clathrate hydrate of formaldehyde, *J. Phys. Chem.*, *100*, 13,330, 1996.

Ritzhaupt, G, and J. P. Devlin, Infrared spectrum of D_2O vibrationally decoupled in glassy H_2O, *J. Chem. Phys.*, *67*, 4779, 1977.

Ritzhaupt, G., C. Thornton, and J P. Devlin, Infrared spectrum of D_2O vibrationally decoupled in H_2O ice Ic, *Chem. Phys. Lett.*, *59*, 420, 1978.

Ritzhaupt, G., W. B. Collier, C. Thornton, and J. P. Devlin, Decoupled vibrational spectra for H_2O in D_2O ice Ic, *Chem. Phys. Lett.*, *70*, 294, 1980.

Rowland, B., M. Fisher, and J P. Devlin, Probing icy surfaces with the dangling-OH-mode absorption: Large ice clusters and microporous amorphous ice, *J. Chem. Phys.*, *95*, 1378, 1991.

Rowland, B., N. S. Kadagathur, J. P. Devlin, V. Buch, T. Feldmann, and M. J. Wojcik, Infrared spectra of ice surfaces and assignment of surface-localized modes from simulated spectra of cubic ice, *J. Chem. Phys.*, *102*, 8328, 1995.

Sandford, S A., L. J. Allamandola, A. G. G. M.Tielens, and G. J. Valero, Laboratory studies of the infrared spectral properties of CO in astrophysical ices, *Astrophys. J.*, *329*, 498, 1998.

Sceats, M. G., M. Stavola, and S. A Rice, On the role of Fermi resonance in the spectrum of water in its condensed phases. *J. Chem. Phys.*, *71*, 983, 1979.

Scherer, J. R., and R. G. Snyder, Raman intensities of single crystal ice Ih, *J. Chem. Phys.*, *67*, 4794, 1977.

Silva, S C., and J. P. Devlin, Interaction of acetylene, ethylene and benzene with ice surfaces, *J. Phys. Chem.*, *98*, 10,847, 1994.

Sivakumar, T. C., S A. Rice, and M. G. Sceats, Raman spectroscopic studies of the OH stretching region of low density amorphous solid water and of polycrystalline ice Ih, *J. Chem. Phys.*, *69*, 3468, 1978.

Smith, R. S., C. Huang, and B. D. Kay, Evidence for molecular translational diffusion during the crystallization of amorphous solid water, *J. Phys. Chem. B*, *101*, 6123, 1997.

Stevenson, K. P., G. A. Kimmel, Z. Dohnalek, R S. Scott, and B. D. Kay, Controlling the morphology of amorphous solid water, *Science*, *283*, 1505, 1999.

Su, X., L. Lianos, Y. R. Shen, and G. A. Somorjai, Surface-induced ferroelectric ice on Pt(111), *Phys. Rev. Lett.*, *80*, 1533, 1998.

Suga, H., T. Matsuo, and O. Yamamuro, Molecular motion and phase transitions of clathrate hydrates, *Supramol. Chem.*, *1*, 221, 1993

Thompson, W. R., B. G. J. P. T. Murray, B. N. Kare, and C. Sagan, Coloration and darkening of methane clathrate and other ices by charged particle irradiation: Applications to the outer solar system, *J. Geophys. Res.*, *92*, 14,933, 1987.

Toon, O. B., M. A. Tolbert, B. G. Koehler, A. M. Middlebrook, and J. Jordan, Infrared optical constants of H_2O ice, amorphous nitric acid solutions and nitric acid hydrates, *J. Geophys. Res.*, *99*, 25,631, 1994.

Tse, J. S., and D. D. Klug, Comments on "Further evidence for the existence of two kinds of H-bonds in ice Ih" by Li et al., *Phys. Lett. A*, *198*, 464, 1995.

Uras, N., and J. P. Devlin, Rate study of ice particle conversion to ammonia hemihydrate: Hydrate crust nucleation and NH_3 diffusion, *J. Phys. Chem. A*, *104*, 5770, 2000.

Westley, M. S., G. A. Baratta, and R. A. Baragiola, Density and index of refraction of water ice films vapor deposited at low temperatures, *J. Chem. Phys.*, *108*, 3321, 1998.

Whalley, E., A detailed assignment of the O-H stretching bands of ice I, *Can. J. Chem.*, *55*, 3429, 1977.

Witek, H, and V. Buch, Structure of ice multilayers on metals, *J. Chem. Phys.*, *110*, 3168, 1999.

Wojcik, M. J., V. Buch, and J. P. Devlin, Spectra of isotopic ice mixtures, *J. Chem. Phys.*, *99*, 2332, 1993.

Wooldridge, P. J., and J. P. Devlin, Proton trapping and defect energetics in ice from FT-IR monitoring of photoinduced isotopic exchange of isolated D_2O, *J. Chem. Phys.*, *88*, 3086, 1988.

Wooldridge, P. J., H. H. Richardson, and J. P. Devlin, Mobile Bjerrum defects: A criterion for ice-like crystal growth, J. *Chem. Phys.*, *87*, 4126, 1987.

Zondlo, M. A., T. B. Onasch, M. S. Warshawsky, M. A. Tolbert, G. Mallick, P Arentz, and M. S. Robinson, Experimental studies of vapor-deposited water-ice films using grazing-angle FTIR-reflection absorption spectroscopy, *J. Phys. Chem. B*, *101*, 10,887, 1997.

J. P. Devlin, Department of Chemistry, Oklahoma State University, Stillwater, OK 74078 (devlin@okstate.edu)

(Received June 21, 2000; revised November 3, 2000; accepted November 27, 2000.)